1 **A Roadmap for Improving the Representation of Photosynthesis in Earth System Models**

2

3 Alistair Rogers[1], Belinda E. Medlyn[2], Jeffrey S. Dukes[3], Gordon Bonan[4], Susanne von
4 Caemmerer[5], Michael C. Dietze[6], Jens Kattge[7,8], Andrew D.B. Leakey[9], Lina M Mercado[10,11], Ülo
5 Niinemets[12] I. Colin Prentice[13,14,15], Shawn P. Serbin[1], Stephen Sitch[10], Danielle A. Way[16], Sönke
6 Zaehle[17]

7 [1]Environmental and Climate Sciences Department, Brookhaven National Laboratory, Upton, NY
8 11973-5000, USA
9 [2]Hawkesbury Institute for the Environment, University of Western Sydney, Locked Bag 1797,
10 Penrith NSW 2751, Australia
11 [3]Department of Forestry and Natural Resources and Department of Biological Sciences, Purdue
12 University, West Lafayette, IN 47907-2061, USA
13 [4]National Center for Atmospheric Research, Boulder, CO 80307-3000, USA
14 [5]Research School of Biology, College of Medicine, Biology and the Environment, Linnaeus
15 Building (Bldg 134) Linnaeus Way, The Australian National University, Canberra ACT 0200
16 Australia
17 [6]Department of Earth and Environment, Boston University, Boston, MA 02215, USA
18 [7]Max Planck Institute for Biogeochemistry, 07701, Jena, Germany.
19 [8]German Centre for Integrative Biodiversity Research (iDiv) Halle-Jena-Leipzig, Deutscher Platz
20 5e, 04103 Leipzig, Germany
21 [9]Department of Plant Biology and Institute for Genomic Biology, University of Illinois at Urbana-
22 Champaign, IL 61801, USA
23 [10]Geography Department, College of life and Environmental Sciences, University of Exeter,
24 Exeter, EX4 4SB, UK
25 [11] Centre for Ecology and Hydrology, Wallingford, OX10 8BB, UK
26 [12]Department of Plant Physiology, Estonian University of Life Sciences, Kreutzwaldi 1, 51014
27 Tartu, Estonia
28 [13]AXA Chair of Biosphere and Climate Impacts, Grand Challenges in Ecosystems and the
29 Environment and Grantham Institute for Climate Change, Department of Life Sciences, Imperial
30 College London, Silwood Park Campus, Buckhurst Road, Ascot SL5 7PY, UK
31 [14]Department of Biological Sciences, Macquarie University, North Ryde, NSW 2109, Australia
32 [15]State Key Laboratory of Soil Erosion and Dryland Farming on the Loess Plateau, College of
33 Forestry, Northwest Agriculture & Forestry University, Yangling 712100, China
34 [16]Department of Biology, University of Western Ontario, London, ON, Canada, N6A 5B7 and
35 Nicholas School of the Environment, Duke University, Durham, NC, USA 27708
36 [17]Biogeochemical Integration Department, Max Planck Institute for Biogeochemistry, Hans-
37 Knöll-Str. 10, 07745 Jena, Germany

38   **Corresponding Author**

39   Alistair Rogers

40   Environmental and Climate Sciences Department

41   Brookhaven National Laboratory

42   Upton, NY 11973-5000

43   USA

44   arogers@bnl.gov

45   +1 631 344 2948

46

Section	Word Count
Main Body	9912
Introduction	554
Representation of Leaf photosynthesis in Terrestrial Biosphere Models	5472
Scaling physiology	3575
Conclusion	320
Acknowledgements	100
Number of Figures	6 (all in color)
Number of Tables	2
Supporting Information	0

47

48   **Summary**

49

50   ● Accurate representation of photosynthesis in terrestrial biosphere models (TBMs) is

51   essential for robust projections of global change. However, current representations

52   vary markedly between TBMs, contributing uncertainty to projections of global carbon

53   fluxes.

54   ● Here we compared the representation of photosynthesis in seven TBMs by examining

55   leaf and canopy level responses of A to key environmental variables: light, temperature,

56   carbon dioxide concentration, vapor pressure deficit and soil water content.

57   ● We identified research areas where limited process knowledge prevents inclusion of

58   physiological phenomena in current TBMs and research areas where data are urgently

59   needed for model parameterization or evaluation.

60   ● We provide a roadmap for new science needed to improve the representation of

61   photosynthesis in the next generation of terrestrial biosphere and Earth System Models.

62

Introduction

66   Fossil energy use is the dominant driver of the increase in atmospheric CO_2 concentration (C_a)

67   and the principal cause of global climate change (IPCC, 2013). Many of the observed and

68   projected impacts of rising C_a portend increasing environmental and economic risk, yet the

69   uncertainty surrounding the projection of our future climate by Earth System Models (ESMs) is

70   unacceptably high (Friedlingstein *et al.*, 2006, Friedlingstein *et al.*, 2014).

71

72   Although CO_2 emissions associated with anthropogenic activity are notable (11 Pg C year^{-1}),

73   they represent less than 10% of the gross carbon fluxes between the land surface and the

74   atmosphere (Beer *et al.*, 2010, Boden *et al.*, 2013, Le Quéré *et al.*, 2015).   Terrestrial

75   photosynthetic CO_2 assimilation (*A*) is the largest of these CO_2 fluxes (~120 Pg C year^{-1}),

76   subsidizing our use of fossil fuels through the net assimilation of about one-third of the CO_2

77   emissions associated with anthropogenic activities (Le Quéré *et al.*, 2015). However, there is

78   critical uncertainty about how the terrestrial carbon sink will be affected by changes in *A* with

79   rising C_a, temperature and drought (Friedlingstein *et al.*, 2014, Gregory *et al.*, 2009, IPCC 2013).

80   Therefore, reducing the uncertainty associated with model representation of *A* is an essential

81   part of improving confidence in projections of global change (Ciais *et al*., 2013).

82

83   In this study we have focused on photosynthesis, but recognize that improving the

84   understanding and projection of the terrestrial biosphere's response to global change also

85   depends on realistically representing many additional processes that are down stream of

86   carbon assimilation (e.g. carbon allocation, plant and soil respiration, and nutrient cycling). Of

87   particularly relevance to photosynthesis is the allocation of extra carbon to leaf area in trees

88   grown at elevated C_a (Ainsworth & Long, 2005). Model representation and integration of these

89   processes, and how the balance between them shifts in their individual and combined

90   responses to environmental drivers, will also be critical in order to capture whole system

91   responses, but such a comprehensive discussion is beyond the scope of this study.

92

93   We examined model representations of A in seven Terrestrial Biosphere Models (TBMs). These

94   models include four that represent the land component of ESMs which were part of the recent

95   Coupled Model Intercomparison Project (CMIP5) - the main resource for the IPCC Fifth

96   Assessment Report (Friedlingstein *et al.*, 2014, IPCC, 2013). Our approach focuses on how

97   physiological responses are represented by TBMs. We compared modeled responses of A to

98   key environmental variables in order to identify areas of model divergence that reflect gaps in

99   current understanding of the physiological and environmental controls of A. In the second half

100   of the paper, we turn to issues of scale - vertical, horizontal and temporal - and consider how

101   representation and parameterization of leaf-level processes is scaled to the canopy within

102   current model frameworks.

103

104   We had three goals: (1) understand how models differ in their representation of A; (2) identify

105   gaps in current understanding of A that contribute to uncertainty in model output; (3) identify

106   areas where current process knowledge and emerging data sets can be used to improve model

107   skill. This study provides recommendations for immediate improvements that can be made to

108   current model representation of *A* and also highlights the scientific activity needed to further

109   advance representation of *A* in the next generation of TBMs.

110

111   **Representation of Leaf Photosynthesis in Terrestrial Biosphere Models**

112

113   **Current model structure and parameterization**

114

115   The Farquhar, von Caemmerer and Berry (FvCB) model of *A* (Farquhar *et al.*, 1980, von

116   Caemmerer, 2000, von Caemmerer & Farquhar, 1981) provides a robust mechanistic

117   representation of *A* in C_3 species, and is the foundation for model estimation of gross primary

118   production (GPP) in many TBMs (Cramer *et al.*, 2001, Rogers, 2014), including the seven models

119   considered here (BETHY, CLM, ED2, G'DAY, JSBACH, JULES and O-CN; Table 1). The formulations

120   of the FvCB model used in these TBMs include elements of; Collatz *et al.* (1991), in CLM, ED2

121   and JULES; Foley *et al* (1996), in ED2; and Kull & Kruijt (1998), in O-CN (Table 1). The FvCB

122   model represents photosynthetic CO_2 assimilation as the most limiting of two biochemical

123   processes: Rubisco carboxylation, and ribulose-1,5-bisphosphate (RuBP) regeneration driven by

124   electron transport. These processes limit *A* in most environments; however, Sharkey (1985)

125   subsequently described how limitations on triose phosphate utilization (TPU limitation) could

126   also limit *A* under some conditions. Only two models in this study included TPU limitation (CLM

127   and JULES, Table 1).

128

129   Similar biochemical models have been developed for the C_4 photosynthetic pathway (von

130   Caemmerer et al. 2000). For reasons of space, we limit our discussion to model treatment of C_3

131   photosynthesis. However we note that a similar exercise focused on C_4 photosynthesis would

132   be valuable.

133

134   Models typically represent stomatal conductance (g_s) using a coupled relationship with A that

135   varies with atmospheric, or leaf-surface, CO_2 concentration, and some measure of atmospheric

136   humidity. This model approach was originally formulated by Ball *et al*. (1987), who used a direct

137   dependence on relative humidity (*RH*) in their equation for g_s. Ball *et al*.'s equation is still

138   widely used in many TBMs, including CLM. Leuning (1995) suggested an alternative equation

139   that depends on vapor pressure deficit (*VPD*) rather than *RH*. ED2 uses the Leuning (1995)

140   equation, while JULES uses a very similar equation developed by Jacobs (1994). The approaches

141   to represent g_s implemented by the models considered here are quite diverse (Table 1) which

142   has a wide-ranging impact on the model outputs we considered.

143

144   The TBMs in this study represent vegetation using broad plant functional types (PFTs). The

145   FvCB model is parameterized with a number of important constants that are typically the same

146   for all PFTs. PFTs are distinguished with respect to photosynthesis through differences in the

147   estimates of the maximum carboxylation rate of Rubisco ($V_{c,max}$), the maximum rate of electron

148   transport (J_{max}) and the slope of the stomatal conductance response. Several groups are now

149   working towards next-generation vegetation models in which PFTs are replaced by "trait-based

150   approaches" (Wullschleger *et al.* 2014). This catchall phrase includes leveraging trait-

151   environment linkages (Ali et al. 2015, Reich 2014, van Bodegom et al. 2014), optimality

152   approaches (Xu et al. 2012, Meir et al. 2015), trait filtering (Fisher et al. 2012) and adaptive

153   global vegetation models (Scheiter et al. 2013). However, our review is relevant to these

154   approaches as well, as they still employ similar representations of photosynthesis. The key

155   difference lies in parameterization, which we discuss when considering scaling to landscapes.

156

157   **Mesophyll conductance**

158

159   In C_3 species, mesophyll conductance (g_m) describes the conductance to CO_2 diffusion from the

160   intercellular airspace within a leaf to the sites of carboxylation within chloroplasts (Flexas *et al.*,

161   2012, von Caemmerer & Evans, 1991). It is one of the four main physiological processes limiting

162   CO_2 uptake and fixation, the others being g_s and the biochemical activity of Rubisco and RuBP

163   regeneration. To our knowledge, there are no land models that currently contribute to the IPCC

164   assessments that consider g_m. This absence reflects the challenge of adding further complexity

165   to the models, but also the uncertainty and technical difficulty of the measurements required

166   to estimate g_m.

167

168   Response curves of A to intercellular [CO_2] (C_i) are routinely used to infer the maximum

169   biochemical activity of Rubisco and RuBP regeneration, i.e. $V_{c,max}$ and J_{max}. When the FvCB

170   model was conceived, the assumption was made that the difference between C_i and the [CO_2]

171   within the chloroplast (C_c) was sufficiently small that it could be ignored. Subsequently,

172   improved measurement techniques for g_m have shown that it can impose a significant

8

173   limitation on A which varies with temperature, and there are significant species differences in

174   these responses (von Caemmerer & Evans, 2015). If g_m is not taken into account in the analysis

175   of A-C_i curves, the true $V_{c,max}$ will be underestimated (Niinemets et $al.$, 2009, Sun et $al.$, 2014,

176   von Caemmerer, 2000). Furthermore, temperature responses of $V_{c,max}$ and J_{max} derived from

177   gas exchange measurements will not necessarily reflect the temperature dependence of the

178   underlying biochemistry alone, but will also reflect the temperature response of g_m (Medlyn et

179    $al.$, 2002a). The use of apparent parameters is problematic if modelers wish to incorporate new

180   data on the underlying biochemistry of photosynthesis. For example, a recent biochemical

181   survey of the catalytic diversity in Rubisco revealed significant and marked variation in key

182   parameters across 75 species (Orr et al. 2016). These data cannot be used directly in models

183   without including g_m in model structures, highlighting the need for improved understanding

184   and model representation of g_m.

185

186   Several TBMs currently use linear relationships between apparent $V_{c,max}$ (obtained from A-C_i

187   curves) and leaf nitrogen to derive $V_{c,max}$ prognostically. If g_m were to be incorporated into

188   future TBMs, new algorithms linking $V_{c,max}$ to leaf N content would be required as the $V_{c,max}$

189   used in the relationship would need to be derived as a function of C_c not C_i. Currently a

190   reliance on apparent V_{cmax} - leaf N relationships means that models underestimate the amount

191   of N partitioned to Rubisco, or put another way, overestimate the nitrogen use efficiency of

192   CO_2 carboxylation by Rubisco.

193

194 It is clear that an improved understanding of g_m remains a critical research area. Despite recent

195 important progress that may simplify prediction of g_m (Tholen *et al.* 2012), we feel that

196 immediate inclusion of g_m in TBMs is premature. "Apparent" parameters derived from A-C_i

197 response curves, which implicitly account for g_m, have been used successfully to model A in

198 many ecosystems at the leaf and canopy level (e.g. Bernacchi *et al.* 2003; Medlyn *et al.* 2005;

199 Thum *et al.* 2007). Until understanding and measurement of g_m matures, its inclusion in TBMs

200 will likely drive additional uncertainty. Furthermore, the modeling community currently has

201 access to a substantial dataset (albeit heavily biased to the mid-latitudes) of "apparent"

202 parameters but almost no data for $V_{c,max}$ and J_{max} derived from A-C_c curves. Including g_m now

203 would dramatically shrink the amount of data available for model parameterization. However,

204 it is important to note that inclusion of g_m in models is essential if carbon isotope

205 discrimination is to be inferred (Ethier & Livingston, 2004; Suits *et al.* 2005).

206 *Recommendation: (1) Greater process knowledge of g_m will be required before it can be*

207 *included in TBMs. Specific needs include improved understanding of variation in g_m across PFTs*

208 *and how it is affected by environmental drivers such as light and temperature.*

209

210 **Short-term leaf level responses to environmental variables in current model structures**

211

212 Our goal was to understand and compare the physiological responses inside these seven TBMs

213 (Table 1). We focused on one particular PFT - a broad leaved deciduous tree - and defined

214 several environmental and physiological variables which provided standard conditions for

215 model intercomparison: instantaneous quantum flux density (Q) = 1500 µmol mol^{-1}, upper

216   canopy sunlit leaf temperature = 25°C, C_a = 380 µmol mol^{-1}, $[O_2]$ = 210 mmol mol^{-1}, VPD = 1

217   kPa, soil moisture content at field capacity and $V_{c,max}$ = 60 µmol m^{-2} s^{-1}. In the following sections

218   we present and discuss leaf level responses to light, temperature, C_a, VPD and soil water

219   content.

220

221   **Short-term response to light**

222

223   The initial slope of the photosynthetic light response curve is determined by the maximum

224   quantum yield of CO_2 assimilation. For clarity, here we distinguish between the *intrinsic*

225   quantum yield (Φ_{int}), which is the initial slope of the relationship between A and absorbed Q

226   under non-photorespiratory conditions and the *realized* quantum yield (Φ_{real}), which we define

227   as the photosynthetic rate per unit incident light at Q = 100 µmol m^{-2} s^{-1} in our standard

228   conditions (Table 2 and the initial slope of the A-Q response in Fig. 1a). The Φ_{int} is generally an

229   input parameter to the models (Table 2) whereas the realized quantum yield is calculated by

230   the models using the FvCB equations, and depends not only on the Φ_{int} but also on the

231   assumed values for the Rubisco kinetic constant Γ^* (the CO_2 compensation point in the absence

232   of mitochondrial respiration), the low light C_i, the leaf absorptance (a), and the convexity of the

233   light response curve (Θ). Model variation in the choice of kinetic constants, low light C_i, a and Θ

234   are summarized in Table 2. The CLM model assumes that Φ_{int} is equal to the theoretical

235   maximum of $(1-f)/8$, where f=0.15 and is used to correct for the spectral quality of light (von

236   Caemmerer, 2000). As a result, CLM has the highest Φ_{real} (0.053 mol mol^{-1}, Table 2, Fig. 1a).

237   The other models are parameterized with quantum yield inputs that result in a calculated Φ_{int}

11

238 that is below the theoretical maximum and the resulting values for Φ_{real} are lower than those

239 for CLM (Table 2). Despite a parameterization that is broadly consistent with other models, the

240 initial slope of the A-Q response of O-CN is strikingly low and results from a limitation of A by

241 light harvesting at low Q (Kull & Kruijt, 1998; Table 1).

242

243 Experimental studies focused on understanding natural variation in quantum yield have shown

244 that there is little variation in Φ_{int} under unstressed conditions across a wide range of species,

245 with an average value of 0.092 mol mol^{-1} (Long *et al*. 1993; Singsaas, Ort & DeLucia, 2001),

246 comparable with the range of Φ_{int} used in the models considered here (0.07 – 0.106, Table 2).

247 However, Φ_{int} can be substantially lower in the field, particularly in stressed conditions (Medlyn

248 *et al* 2007; Niinemets *et al*. 2004, 2014; Singsaas, Ort & DeLucia, 2001). As discussed above, the

249 Φ_{real} in models depends on several assumptions, not just the Φ_{int}, highlighting the need to

250 better parameterize and test modelled light responses with data from field conditions. For

251 example, most existing measurements have been made within a narrow temperature range (20

252 – 30°C) and the scarcity of data collected at low temperature has been highlighted as an

253 important driver of model uncertainty at high latitudes (Dietze *et al*., 2014).

254

255 Leaf level light-saturated CO_2 uptake (A_{sat}) varies considerably between models (Fig 1a). The

256 variation in modelled A_{sat} is driven by differences in prescribed Rubisco kinetic constants and

257 their temperature dependencies (see below and Table 2), as well as the C_i, which is dependent

258 on the choice of stomatal model. The inflection point of the light response curve marks the

259 transition between light limitation and light saturation of A. There is a wide range in the Q at

260   which *A* becomes light saturated and therefore the greatest model divergence in *A* occurs when

261   some models have light saturated *A* and others do not (i.e. *Q* = 400-800 µmol m^{-2} s^{-1}, Fig. 1). In

262   addition to differences in the model representation of light limited and light saturated *A,*

263   variation in the transition phase is attributable to model structure (Table 1), and when present,

264   parameterization of the convexity term (*Θ*, Table 2), which determines the relative influence of

265    $Φ_{real}$ or A_{sat} on *A* at a given *Q*.

266

267   Moving from the leaf to the canopy level, responses to irradiance (Fig 1, b-d) are not only

268   dependent on the factors discussed above but also on the method used to scale physiology

269   from the leaf to the canopy level, the representation of the light environment within the

270   canopy, and the partitioning of foliage between sunlit and shaded leaves (Gu *et al.* 2002,

271   Mercado *et al.* 2009). As a result, canopy scaling exacerbates existing differences between the

272   TBMs and introduces new structural variation that further diversifies model output (Fig. 1 b-d).

273   Canopy scaling is discussed in detail below.

274   *Recommendation: (2) Modeled responses of photosynthesis to light need to be parameterized*

275   *and evaluated against data from field conditions, particularly at low temperature.*

276

277   *Don't mix & match*

278   One issue that emerged here, but is relevant throughout this paper, is the need to avoid

279   piecemeal approaches to model parameterization. For example, we need to carefully and

280   consistently use kinetic constants and temperature response functions because the models are

281   highly sensitive to them. Any constants and functions used when deriving photosynthetic

282 parameters from data have to be the *same ones* used in the model. For example, if a value of

283 $V_{c,max}$ at 25°C is used in a model, that model must use the same Michaelis-Menten constants (K_c

284 and K_o) and Γ^* (e.g. see Table 2), and the associated temperature dependencies, that were

285 used to estimate $V_{c,max}$ from the original A-C_i response curve as well as the same temperature

286 response function (e.g. see Table 1) used to scale $V_{c,max}$ from the measurement temperature to

287 25°C. This problem, that derived parameters depend on the equations used to derive them,

288 introduces error when trying use the parameters to perform meta-analyses or calibrate models

289 (Medlyn *et al*. 2002, Dietze 2014). As we make progress to provide models with richer data sets

290 for use in model parameterization and evaluation, we need to archive our raw gas exchange

291 data so that, for example, new kinetic constants and temperature response functions can be

292 applied to old data, maintaining its value as understanding advances. The estimation of

293 quantum yield provides another example where the assembly of parameters (e.g. Φ_{int}, a, Γ^*, Θ)

294 and approaches (e.g. estimation of low light C_i) is not coordinated and where archived data

295 would be useful.

296 *Recommendations: (3) Models need to make careful and consistent use of kinetic constants and*

297 *temperature response functions. (4) Physiologists should archive their raw data to enable*

298 *coordinated parameterization and the preservation of their data for future analysis.*

299

300 **Short-term response to temperature**

301

302 The temperature response of A is complex and dependent on additional variables such as Q and

303 C_i (Fig 2). The C_i in turn depends on g_s and hence *VPD*, such that the temperature and *VPD*

14

304 response of g_s also impacts the shape of the temperature response of A (Medlyn *et al.*, 2002a;

305 Lin *et al.*, 2012). The model by Farquhar *et al*. (1980) suggests that A is Rubisco-limited at low

306 temperature - but note that TPU limitation can limit A in some species at low temperature

307 (Sage & Sharkey, 1987). The decline in A at high temperature (Fig. 2) can be brought about by

308 the temperature dependence of J_{max} and the strong increase in photorespiration and

309 mitochondrial respiration with increasing temperature (Farquhar *et al.*, 1980; von Caemmerer,

310 2000). High temperature limitations on Rubisco activase could also cause decline in A but this

311 mechanism is currently absent from all these models (Salvucci & Crafts-Brandner 2004a;

312 Salvucci & Crafts-Brandner 2004b, Sage & Kubien 2007). The steep decline of A at temperatures

313 above 30°C in the Farquhar *et al.* (1980) model is largely driven by the temperature

314 dependence of J_{max}. This effect needs to be treated with some caution as it may be due to

315 irreversible inhibition in the *in vitro* system, from which the function was derived. June *et al*.

316 (2004) provided a simpler empirical equation for fitting the temperature dependence of J_{max}.

317 The temperature dependence of A is also driven by the choice of kinetic parameters and their

318 temperature dependencies as discussed above. Some TBMs use spinach (Jordan and Ogren

319 1984) or tobacco (Bernacchi *et al*. 2001) temperature response functions for $V_{c,max}$ for all

320 species. However, as there are important differences in the response of $V_{c,max}$ to temperature

321 among warm and cool climate plant species (Kattge & Knorr 2007; Galmes *et al*. 2015),

322 continued acquisition of temperature response functions from different biomes is critically

323 important. The temperature optimum of A (T_{opt}) depends on environmental conditions such as

324 Q and C_a, with T_{opt} being more pronounced at high Q and C_a (e.g. compare Figs 2a & c with 2b

325 & dd). Here, two models stand out for their temperature responses; unlike the majority of

326   models that show an optimum ~24.5^{o}C, ED2 has an emergent temperature optimum at 16°C,

327   despite a $V_{c,max}$ optimum at 39°C, and JSBACH shows no high temperature limitation on A

328   (Table 1, Fig 2). It is usual for T_{opt} to shift to a slightly higher temperature as C_a rises (Long,

329   1991) because at high C_a the rate of photorespiration is reduced, thereby extending the

330   temperature range where positive CO_2 assimilation occurs. The CO_2 effect on T_{opt} is evident in

331   Fig. 2 in a number of the models at both the leaf and canopy level. Here, elevating C_a from 380

332   to 550 μmol mol^{-1} shifts the T_{opt} up by ~2°C (Fig 2 b,d). Two models do not show this shift in

333   T_{opt}: JSBACH has no T_{opt}, and the T_{opt} for ED2 remains at 16°C despite the increase in C_a from

334   380 to 550 μmol mol^{-1}.

335

336   Current empirical models predict the response of g_s to temperature based on a relationship

337   between g_s and A that is modified by VPD. This approach is successful in many cases (e.g.

338   Duursma et al. 2014) although the mechanisms underlying the response remain poorly

339   understood (Mott, 2009; Busch, 2013). In addition, there is evidence that the correlation

340   between g_s and A breaks down at high temperatures (> 35°C) in some species, with stomata

341   remaining open while A goes to zero (e.g. Lu et al. 2000; Scafaro et al. 2012; Slot et al. 2016;

342   Teskey et al. 2015; von Caemmerer and Evans 2015). Presumably this response allows the plant

343   to maintain leaf temperatures at non-damaging levels via transpirational cooling. It is not

344   known how widespread this response is (Teskey et al. 2015) nor to what extent it occurs in the

345   field. Slot et al. (2016), for example, find this response in glasshouse-based measurements but

346   not in field trees.

347   *Recommendations: (5) Physiologists need to continue measuring temperature response*

348   *functions for $V_{c,max}$ and J_{max}. (6) More field-based research into the independent temperature*

349   *response of g_s is required to better understand the mechanism underlying the response of A to*

350   *high temperatures.*

351

352   **Short-term response to CO_2**

353

354   At low C_a, when A is limited by the amount of active Rubisco available for carboxylation ($V_{c,max}$),

355   A increases with rising C_a for two reasons: (1) the affinity of Rubisco for CO_2 is low, and

356   therefore increasing the substrate concentration increases carboxylation rates; (2) CO_2

357   competitively inhibits the oxygenation reaction, reducing CO_2 losses associated with

358   photorespiration (Fig. 3). At higher C_a - i.e. above the inflection point of the A-C_a curve (most

359   notable in the leaf level responses shown in Figs 3a & b) - A becomes limited by the supply of

360   ATP and NADPH to regenerate the CO_2 acceptor RuBP. At this point A will still rise with

361   increasing C_a, but the CO_2 responsiveness (the increase in A for a given increase in C_a) is

362   reduced as further increases in A are attributable solely to the inhibition of the oxygenation

363   reaction, which increases the availability of ATP and NADPH for RuBP regeneration (Long 1991,

364   Long *et al.* 2004).

365

366   The shape of the A- C_a response curve is a critical model feature that determines the ability of

367   the terrestrial carbon sink to respond to rising C_a and it is affected by model structure and

368   parameterization (Fig. 3, Tables 1 & 2). Variation in the initial slope of the A-C_a response is

369   attributable to C_i and the choice of kinetic constants. For this example of a broad leafed

370   deciduous tree PFT in our standard conditions, all models show that light-saturated A appears

371   to be Rubisco limited (RuBP saturated) below a C_a of 500 µmol mol^{-1} (Fig. 3). As a result the CO_2

372   responsiveness of A below a C_a of 500 µmol mol^{-1} is similar for all models. However, as C_a rises

373   above 500 µmol mol^{-1} differences in model structure and parameterization lead to substantial

374   variation in CO_2 responsiveness. Three models (CLM, ED2 and JULES) stand out for smooth

375   response curves that lack a clear inflection point (most noticeable in Fig 3a). All three models

376   adopt the co-limitation approach described by Collatz *et al.* (1991) which smooths transitions

377   between Rubisco limited and RuBP limited A (Collatz *et al.* 1991; Foley *et al*. 1996; Clark *et al*.

378   2011; Oleson *et al*. 2013, Table 1). This approach contributes to the greater CO_2

379   responsiveness at higher C_a observed in CLM and JULES (Fig 3a). In addition, the four models

380   that lack this smoothing function (BETHY, G'DAY, JSBACH and O-CN) have a marked inflection

381   point between Rubisco limited and RuBP limited A, but the C_a at which this inflection occurs

382   spans a large range (~300 µmol mol^{-1}, Fig. 3) contributing to the variation in CO_2 responsiveness

383   above 500 µmol mol^{-1}. The variation in C_a at which the inflection point occurs has several

384   causes, but the main drivers of this variation are the choice of kinetic constants (~60 µmol mol^{-}

385   ^{1}, Table 2), the JV_{ratio}, which for a fixed $V_{c,max}$ sets the inflection point C_i (~125 µmol mol^{-1}, Table

386   2) and the stomatal model, which determines the C_a at which the inflection point C_i is reached

387   (~175 µmol mol^{-1}, Table 1).

388

389   As $V_{c,max}$ is reduced (Fig. 3b, 3d), the responses of A to changes in C_a are qualitatively similar

390   but model divergence is constrained. Model variation in canopy level responses to rising C_a (Fig

391   3c & d) is also attributable to different approaches to canopy scaling as discussed below. The

392   differences seen here in CO_2 responsiveness are substantial - highlighting the impact of

393   different model representations of the FvCB equations, stomatal model choices and the need to

394   better understand controls on the inflection point of the A-C_a response. The C_a at which the

395   inflection point occurs drives uncertainty in the CO_2 stimulation of A at the C_a that will be

396   experienced in the second half of the century, and it is at this higher C_a where model

397   uncertainty is greatest. This effect probably contributes to the model differences in *GPP*

398   reported in the recent FACE model-intercomparison project (Zaehle *et al.* 2014).

399   *Recommendation: (7) We need improved understanding and model evaluation of the controls*

400   *on the inflection point of CO_2 response curves.*

401

402   **Short-term response to VPD**

403   Increasing *VPD* causes stomatal closure, which decreases C_i . The magnitude of the decrease in

404   A resulting from lower C_i is determined by the shape of the A-C_i response as described above

405   and shown in Fig. 3. Figure 4 shows the response of A to *VPD;* model divergence increases with

406   rising *VPD*, largely due to differences in the parameterization of *VPD* sensitivity among models .

407   The strong sensitivity of the CLM model seen in Figure 4 is due to the use of *RH* in the model

408   formulation, and the fact that RH must drop dramatically to obtain increasing *VPD* with

409   constant temperature, as shown in this plot. There are some models, of which JSBACH in this

410   study is an example, that do not incorporate a stomatal response to *RH* or *VPD* (Table 1, Figure

411   4). Such formulations were necessary when driving data sets for atmospheric humidity were

412   not available. Given advances in the understanding of stomatal responses and the availability

19

413   of appropriate driver datasets, stomatal response to *RH* or *VPD* should be adopted. However,

414   we believe that formulations involving *VPD*, such as those adopted by ED2, G'DAY and JULES

415   (Table 1) are theoretically preferable because, unlike *RH*, *VPD* is directly proportional to water

416   loss, more closely reflects stomatal mechanics (e.g. Aphalo & Jarvis 1991; de Beeck, 2010), and

417   is strongly linked to productivity (Lobell *et al*. 2014; Ort & Long, 2014). In addition, formulations

418   involving *VPD,* rather than *RH,* will likely be better able to project the response of vegetation to

419   future climate scenarios, because *RH* is predicted to change little in the future whereas *VPD* will

420   increase with warming (Sato *et al*. 2015).

421

422   Similar coupled g_s-*A* models can also be developed from optimization principles. Cowan &

423   Farquhar (1977) proposed that stomatal behavior is optimal when *A* less the cost of

424   transpiration is maximized, and a number of authors have shown that this theory leads to a

425   relationship between g_s and *A* that is similar in behavior to empirical formulations (e.g. Hari *et*

426   *al*. 1986; Katul *et al*. 2010; Medlyn *et al*. 2011). Optimization approaches have the advantage of

427   being based in theory, yielding meaningful parameter values, and providing g_s responses to

428   future environmental conditions where we lack robust measurements, and we encourage their

429   use. However, we also caution that optimization can lead to physiologically incorrect behavior

430   in some circumstances – such as incorrect CO_2 responses, and instability near the transition

431   between Rubisco-limited and RuBP regeneration-limited *A* – implying that simple, empirically

432   verified equations based on optimization may be more reliable than direct application of

433   numerical optimizations that are also dependent on the careful application of model

434   constraints within TBMs and the optimization approach used.

435

436   Large-scale parameterization of stomatal models has been data-limited, with models typically

437   using one nominal set of parameter values for all C_3 vegetation. A major advance in this area

438   was made by Lin *et al*. (2015), who collated a substantial new stomatal conductance database

439   and demonstrated a predicted response of the stomatal slope parameter (g_1) to temperature

440   and consistent differences in g_1 among broadly defined PFTs. This dataset provides a valuable

441   foundation for stomatal model parameterization. However, the coverage of this database is still

442   limited.   There is still relatively little information about how g_1 varies among species or

443   genotype, and almost no information on acclimation or plasticity in these parameters in

444   response to abiotic or biotic factors (Way *et al*. 2011). Models are also sensitive to the

445   minimum stomatal conductance parameter, g_0, particularly under low light and high *VPD*

446   conditions (Bauerle *et al*. 2014), but this parameter is poorly quantified.

447   *Recommendation: (8) Models should adopt approaches that include formulations where g_s*

448   *responds to VPD. (9) We need more information about how g_1 and g_0 (or their equivalents) vary*

449   *among PFTs and in response to environmental drivers.*

450

451   **Short-term response to Soil Moisture Content**

452

453   Soil moisture availability is a key constraint on *A*. As soil moisture availability decreases,

454   stomates close, decreasing C_i, and eventually preventing *A* and transpiration (Fig. 5). Drought

455   can also reduce the biochemical capacity for *A*, expressed as lower $V_{c,max}$ and J_{max} in models,

456   but the relative balance of these stomatal and biochemical limitations is subject to significant

457   debate (Chaves *et al* 2009). Current approaches to modelling the effects of soil moisture on A

458   can be classified into several types: empirical reduction factors; hydraulic limitations;

459   physiological approaches; and a simple supply constraint approach (BETHY). The latter assumes

460   that plant transpiration cannot exceed the potential supply of soil water and that plants can

461   photosynthesize provided there is a sufficient water supply (Table 1).

462

463   The empirical reduction factor approach involves multiplying parameters by a soil water stress

464   factor (typically denoted β, ranging from 0 to 1) when soil moisture falls below a given model

465   model-dependent threshold. Three of the models in our sample used this approach (CLM,

466   G'DAY and O-CN, Table 1 & Fig. 5). However, there is disagreement among models as to

467   whether the β factor should be applied to the stomatal slope parameter, apparent $V_{c,max}$, or

468   both (De Kauwe *et al*. 2013). Here, all three models applied the β factor to stomatal model

469   parameters, either the slope (G'DAY and O-CN) or the intercept (CLM), and also to the

470   photosynthetic parameters $V_{c,max}$ (CLM) or $V_{c,max}$ and J_{max} (G'DAY and O-CN, Table 1). Increasing

471   evidence suggests that both stomatal slope and $V_{c,max}$ are affected by low soil moisture, with

472   the reduction in apparent $V_{c,max}$ possibly in part due to lower g_m (Keenan *et al*. 2010; Egea *et al*.

473   2011; Zhou *et al*. 2013). Several TBMs do include both limitations, but the β factor is tied to the

474   soil water content and therefore models cannot capture the impact of potentially different

475   trajectories of drying and rewetting episodes (Williams *et al*. 2009).

476

477   The hydraulic approach offers a number of theoretical advantages over the β-factor approach.

478   Stomatal conductance is modelled as a function of leaf water potential (ψ_{leaf}), which is

479   calculated from soil moisture potential ψ_{soil} and plant and soil hydraulic conductances. There

480   may be a threshold minimum ψ_{leaf} (Williams *et al*. 1996) or a sigmoidal functional dependence

481   (Tuzet *et al*. 2003). Implementations also differ on whether responses to *VPD* are captured by

482   the responses to ψ_{leaf} (Williams *et al*. 1996, Tuzet *et al*. 2003) or whether an additional *VPD*

483   response is also needed (Bonan *et al*. 2014). The hydraulic approach is appealing to plant

484   physiologists because it reflects some of the key mechanisms thought to influence plant

485   response to drought (Leuning *et al*. 2004). Because soil hydraulic conductance is assumed to

486   vary with ψ_{soil} this approach also incorporates a dynamic weighting of soil layers whereby lower

487   soil layers become more important as drought progresses (De Kauwe *et al*. 2015). Furthermore,

488   there is evidence that the photosynthetic response to soil moisture can depend on plant leaf

489   area (e.g. Kelly *et al*. 2015), an effect that is captured by the hydraulic approach but not the β-

490   factor approach. The chief disadvantage of the hydraulic approach is that it requires additional

491   parameters to represent plant hydraulic conductance and stomatal dependence on leaf water

492   potential. These parameters are not well quantified and can lead to additional uncertainty.

493

494   The physiological approaches are based on an understanding of stomatal function and suggest

495   that both metabolic and hydraulic stomatal regulation involves the hormone abscisic acid

496   (*ABA*), known to promote tolerance against abiotic stress (Jones *et al.*, 2015). Wilkinson and

497   Davies (2002) proposed a coordinated model of plant responses to stress whereby water stress

498   sensed by the root system stimulates *ABA* biosynthesis. This signal is then communicated to the

499   guard cells which subsequently induce stomatal closure and reduce water loss. Both roots and

500   leaves synthesize *ABA* and increasing concentrations of xylem *ABA* correlate with stomatal

501   closure (Sauter *et al.*, 2001; Wilkinson and Davies, 2002, Christmann *et al*. 2007).

502

503   There are few mathematical descriptions of stomatal control including xylem *ABA* signaling

504   (Tardieu and Davies, 1993; Dewar, 2002; Huntingford *et al.*, 2015). Tardieu and Davies (1993),

505   combined hydraulic and chemical signaling control of stomatal functioning. The approach of

506   Dewar (2002) is an extension of this approach that also considers xylem embolism and the

507   possible role of combined leaf hydraulic and chemical signaling in addition - or as a possible

508   alternative - to existing root signals. Huntingford *et al.* (2015) revisited the work by Dewar

509   (2002) and provided a g_s formulation which depends on only four variables: soil water content,

510   C_a, evapotranspiration and net *A*. This is an exciting approach, however there is an acute need

511   for more empirical data to be able to parameterize and evaluate approaches of estimating g_s

512   that include *ABA*.

513

514   The TBMs presented here showed dramatic divergence in the response of *A* to drought (Fig. 5),

515   with the canopy level responses mostly mirroring the responses seen at the leaf level. Whilst

516   much of this divergence could be explained by the different approaches taken by each model

517   (Table 1), the method used to estimate soil water availability also varies between models. Some

518   models estimate soil water availability using soil moisture content (e.g. O-CN) and others using

519   ψ_{soil} (e.g. CLM). Since soil water retention curves are highly nonlinear and dependent on soil

520   type, this can be a major source of model divergence (Medlyn *et al.* 2016). From a physiological

521   perspective, ψ_{soil} is thought to be more relevant to plant function than soil moisture content.

522 However, the use of ψ_{soil} can result in unrealistically steep responses to the onset of drought

523 unless it is dynamically averaged over the soil profile (De Kauwe *et al.*, 2016).

524

525 Uncertainties in root and stomatal responses are major drivers of TBM uncertainty in predicted

526 *NPP* across a wide latitudinal gradient (Dietze *et al.* 2014; De Kauwe *et al.* 2013). Improved

527 model representation of drought responses will require evaluation of underlying mechanisms

528 as well as comparison of high level model outputs to ecosystem fluxes during drought periods.

529 Evaluation of the response of key variables associated with alternative stomatal models against

530 field data is needed. This is challenging as evaluation of alternative mechanisms (e.g. the

531 hydraulic and physiological approaches) requires field level manipulation or exploitation of

532 natural gradients and weather events coupled with substantial campaigns that include parallel

533 measurement of many leaf parameters (e.g. ψ_{leaf}, *in situ* gas exchange and $V_{c,max}$) in

534 coordination with plant hydraulic parameters (e.g. soil moisture content, ψ_{soil}, sap flux,

535 hydraulic conductivity and cavitation vulnerability).

536 *Recommendations: (10) Models should respond to soil water availability through ψ_{soil}, but*

537 *variation in ψ_{soil} with soil depth needs to be incorporated (11) We need rich data sets of*

538 *coordinated physiological and environmental measurements to enable evaluation of alternative*

539 *modeling approaches for the representation of the response of A to drought.*

540

541 **Scaling physiology**

542

543   Above, we focused primarily on leaf level responses to environmental and climate change

544   drivers, but a major challenge for model representation is how to scale process knowledge of

545   physiology and leaf level parameterization through time (seasonal change), vertically through

546   the canopy, spatially across the landscape, and also to represent photosynthetic acclimation to

547   rising temperature and C_a. These issues are discussed below.

548

549   **Effects of day length and season**

550

551   Photosynthesis responds to short-term environmental changes, but it also shows broad, regular

552   seasonal changes, especially in higher latitudes. In these regions, A halts in the autumn as

553   leaves senesce in deciduous species and decreases as $V_{c,max}$ is down-regulated during the cold

554   winter months in evergreens. Much of this temporal scaling of A is captured in TBMs through

555   phenology models and the direct temperature effects on $V_{c,max}$.

556

557   While temperature may be a major factor in driving seasonal patterns of A, other

558   environmental cues may be as, or even more, important. Photoperiod is known to have strong

559   effects on leaf phenology, which has indirect effects on A, but has not generally been

560   considered to affect A directly (Way & Montgomery, 2015). However, Bauerle *et al*. (2012)

561   found that photoperiod was a stronger predictor of seasonal changes in both $V_{c,max}$ and J_{max}

562   than air temperature. In that data set, $V_{c,max}$ peaked immediately after the summer solstice,

563   and declined steadily into the autumn, although air temperatures did not peak until a month or

564   more after the solstice. When this effect was accounted for with a photoperiod correction of

565   $V_{c,max}$ in CLM, the model's ability to capture seasonal patterns of atmospheric C_a was improved

566   (Bonan *et al*. 2011; Bauerle *et al*. 2012). Other papers have noted that incorporating a

567   photoperiod scalar with direct effects on $V_{c,max}$ improves estimates of seasonal carbon fluxes in

568   eddy flux studies, supporting a role for photoperiod in modulating $V_{c,max}$ (Medvigy *et al*. 2013;

569   Stoy *et al*. 2014). In controlled environments, photoperiod is tightly correlated with total leaf

570   protein content, suggesting a tradeoff between the value of protein and the cost of its

571   maintenance and provides a possible mechanistic explanation for the impact of photoperiod on

572   $V_{c,max}$ (Hannemann *et al*. 2009). However, not all PFTs show the same response to changes in

573   day length and it is possible that photoperiod corrections may be capturing leaf age effects

574   (Medlyn *et al*. 2002b; Medlyn *et al*. 2007; Busch *et al*. 2007; Lin *et al*. 2013; Stinziano *et al*.

575   2015). In the tropics, day-length is essentially constant and therefore photoperiod scalars will

576   fail to capture the well documented photosynthetic seasonality associated with tropical

577   evergreen forests (Doughty & Goulden, 2008). In dry season Amazonian evergreen forests

578   recent work has shown that a higher canopy level photosynthetic capacity associated with new

579   leaf flushing explains seasonal dynamics of photosynthetic rate (Wu *et al*. 2016a).

580   *Recommendations: (12) We need to elucidate the mechanism underlying the use of photoperiod*

581   *scalars to modify photosynthetic parameterization. (13) In order to capture photosynthetic*

582   *seasonality in tropical evergreen forests, we need to develop new approaches that are capable*

583   *of coupling prognostic leaf phenology to photosynthetic capacity.*

584

585   **Acclimation to temperature**

586

587 The short-term photosynthetic responses to temperature covered above are themselves

588 sensitive to the temperatures experienced over longer time scales (days to weeks). This longer-

589 term adjustment, known as temperature acclimation, has been widely reported and recently

590 reviewed (Smith and Dukes 2013, Way & Yamori 2014). The phenomenon is commonly

591 observed as a shift in the optimum temperature for A (T_{opt}), which can maximize the A at the

592 growth temperature (Berry & Björkman, 1980; Yamori *et al.*, 2014; Kattge & Knorr, 2007). The

593 mechanistic process of acclimation and its timescale have not been well described, either

594 within or across species. At the slowest and broadest scales, the process of acclimation is

595 constrained by leaf structure and rates of leaf development and turnover. Leaves that develop

596 under one set of conditions are constrained by their existing anatomy from adjusting fully to a

597 new set of conditions (Campbell *et al.* 2007). Within a leaf, acclimation rates are driven by the

598 rates at which biochemical and physiological processes can adjust.

599

600 At the leaf scale, acclimation results from temperature-driven changes in enzyme abundances

601 and isoforms, and of membrane composition (Yamori *et al.* 2014). At low growth

602 temperatures, the abundance of Rubisco and other photosynthetic enzymes increases, and

603 some plants produce enzymes with different isoforms, which have different kinetic constants.

604 Under high growth temperatures, plants are thought to increase the stability of the thylakoid

605 membrane, and their capacity for increased electron transport. Also, some plants can produce

606 a more heat-stable form of Rubisco (Crafts-Brandner *et al.* 1997), and increase expression of

607 heat-shock proteins. Growth temperature also affects the temperature response of respiration,

608 with consequences for net A (e.g., Atkin & Tjoelker 2003, Way & Yamori 2014); although the

609   acclimation of respiration may affect plant growth more strongly than that of A for some

610   species (Way & Oren 2010), this topic lies beyond the scope of this paper and has recently been

611   considered elsewhere (Atkin *et al.* 2015).

612

613   While long-term acclimation of A to temperature has been observed in many species and

614   studies, fewer studies have quantified acclimation at the process level i.e. $V_{c,max}$ and J_{max}. From

615   observed responses, one may expect seasonal variation in the temperature dependence of J_{max}

616   and changes in the JV_{ratio}. Some confirmation of this was provided by Kattge & Knorr (2007)

617   who reanalysed data from 36 (primarily temperate) plants and showed that the optimum

618   temperature of $V_{c,max}$ and J_{max} increased by $0.44^{o}C$ and $0.33^{o}C$ per $1^{o}C$ increase of growth

619   temperature, and that the JV_{ratio} at $25^{o}C$ significantly decreased with increasing growth

620   temperature. However, temperature acclimation may result from different processes in

621   different species: $V_{c,max}$ and J_{max} measured at $25^{o}C$ were, on average, unaffected by growth

622   temperature across tree species (Way & Oren, 2010) and showed a wide variation in responses

623   across a broad range of plant growth forms (Way & Yamori 2014).

624

625   The representation of $V_{c,max}$ and J_{max} acclimation based on Kattge & Knorr (2007) has been

626   included in some models (e.g., Raddatz *et al*. 2007, Ziehn *et al*. 2011, Arneth *et al*. 2012,

627   Lombardozzi *et al*. 2015), and recent work suggests that incorporation of both photosynthetic

628   and respiratory acclimation can alter projections of land carbon storage by 10-40 Pg by the end

629   of the century (Lombardozzi *et al*. 2015, Smith *et al*. 2016). However, there is clear indication

630   that species differ in the degree to which they acclimate to temperature (e.g., Yamori *et al*.

631   2014), and no formulations have yet been developed that capture this variation across a broad

632   range of PFTs.

633

634   Researchers have recorded acclimation of different species occurring over periods lasting from

635   two days to nearly two weeks (e.g., Björkman & Badger 1979, Gunderson *et al*. 2010, Slatyer &

636   Ferrar 1977). Very limited evidence suggests that the exact timescale of acclimation may not be

637   critical for modeled estimates of GPP as long as it is in a range of approximately 3-45 days

638   (Dietze 2014) but the issue needs to be evaluated more thoroughly before that assumption is

639   widely adopted. A specific timescale does need to be specified in models to calculate growth

640   temperature, and is straightforward to identify experimentally. Kattge & Knorr (2007) assumed

641   an acclimation period of 30 days, using an average of day and night temperatures, but it is clear

642   that the bulk of biochemical and physiological adjustments happen over a shorter time period.

643   *Recommendations: (14) Physiologists need to measure thermal acclimation of the*

644   *photosynthetic traits (e.g. $V_{c,max}$ and J_{max}) that drive model outputs rather than thermal*

645   *acclimation of A. (15) We need a better understanding and model representation of thermal*

646   *acclimation across biomes, specifically the capacity and degree to which species can acclimate,*

647   *the time scales over which acclimation occurs, and the degree to which temperature acclimation*

648   *is affected by other environmental variables.*

649

650   **Acclimation to rising [CO_2]**

651

652 Photosynthetic acclimation to elevated C_a is the reduced stimulation of A that often occurs

653 following long-term growth at elevated C_a (Ainsworth & Rogers, 2007). It is the result of a

654 reduction in $V_{c,max}$ relative to J_{max} (Ainsworth & Long, 2005, Ainsworth & Rogers, 2007, Leakey

655 *et al.*, 2009, Long *et al.*, 2004, Rogers & Humphries, 2000). Notably, the reduction in

656 photosynthetic capacity typically reduces the magnitude of the stimulation of A without

657 completely eliminating it (Leakey *et al.* 2009). The acclimation response reduces allocation of N

658 to Rubisco, thereby allowing N resources to be combined with the greater C supply from

659 stimulated A at elevated C_a (Drake *et al.* 1997, Long *et al.* 2004). In fact, a meta-analysis of

660 Ainsworth & Long (2005) found that the decrease in leaf N content observed at elevated C_a was

661 largely attributable to the decrease in Rubisco. Consequently, the magnitude of any

662 photosynthetic acclimation is tightly coupled to the C and N status, and the source-sink

663 balance, of the plant (Medlyn, 1998; Ainsworth & Rogers, 2007, Ainsworth *et al.*, 2004, Leakey

664 *et al.*, 2009, Rogers *et al.*, 2009, Rogers *et al.*, 1998). For example, in severely N limited systems,

665 acclimation is strong and can be attributed to a nonspecific reduction in leaf N content (Warren

666 *et al.*, 2015), a mechanism that is currently accounted for by some TBMs in this study (Table 1).

667 Acclimation is also strong when the capacity of sinks to use photoassimilate is low, leading to

668 accumulation of leaf carbohydrates and induction of sugar signaling pathways that reduce

669 expression of Rubisco (Moore *et al.* 1999). There is evidence for variation in the acclimation

670 response among functional groups that differ in the processes limiting A at ambient C_a

671 (Ainsworth & Rogers, 2007). Acclimation is rarely observed in plants that have Rubisco-limited A

672 at current C_a and elevated C_a. As C_i rises above the inflection point on an A-C_i response curve,

673 A will become RuBP regeneration-limited, and carboxylation capacity will exceed requirements.

674   In this situation, plants grown at elevated C_a typically exhibit photosynthetic acclimation and

675   reduce their investment in Rubisco (Ainsworth & Rogers, 2007).

676

677   The TBMs in this review either do not include photosynthetic acclimation to elevated C_a or link

678   it to a non-specific reduction in leaf N content that is focused on reduced N availability and

679   constrained C:N stoichiometry (Luo *et al.*, 2004). No models currently include representation of

680   the physiological acclimation to elevated C_a described above and widely reported in Free Air

681   CO_2 Enrichment (FACE) studies (Long *et al.* 2004, Ainsworth & Rogers 2007, Leakey *et al.* 2009),

682   where the meta-analysis of Ainsworth & Long (2005) found that the decrease in leaf N content

683   observed at elevated C_a was largely attributable to the decrease in Rubisco.   2009). Recent

684   analysis has shown that failing to account for photosynthetic acclimation at elevated C_a leads to

685   an overestimation of yield in soybean (Twine *et al.*, 2013) - a legume where reductions in leaf N

686   content at elevated C_a are theoretically minimal (Rogers *et al.*, 2009). Therefore, the potential

687   for model representation of photosynthetic acclimation to elevated C_a to reduce errors of this

688   type when modeling other more N limited systems is likely substantial. In future TBMs we

689   believe it will be important to capture the mechanisms that control physiological acclimation to

690   rising C_a and not just acclimation resulting from reduced N availability. An approach that

691   reduces N allocation to Rubisco when C_a rises beyond the inflection point of PFT-specific CO_2

692   response curves would be a good first step.   However, unlike thermal acclimation, no

693   algorithms have been developed to facilitate inclusion of this concept in TBMs despite the

694   substantial research from FACE experiments.   Published data from FACE experiments could

695   potentially be used for development and validation of new algorithms.

696 *Recommendation (16) We need to develop a new model representation of the physiological*

697 *acclimation of photosynthesis to elevated C_a.*

698

699 **Leaf to canopy scaling**

700

701 Due to high non-linearity of photosynthetic responses to light, temperature and *VPD*, scaling *A*

702 from leaves to canopy remains an important challenge for models (Jarvis, 1995). Central to this

703 challenge is TBM representation of light penetration and utilization within the canopy's vertical

704 profile and the vertical scaling of physiology within the canopy. Analogous effects arise from

705 within-canopy variations in temperature and *VPD*, although to a lower degree (Niinemets &

706 Anten, 2009).

707

708 Although the average light intensity typically decreases exponentially with increasing

709 cumulative leaf area index through the canopy, the extent of this decline is affected by the

710 optical properties of individual leaves (including albedo) and how these change with canopy

711 depth, season and leaf age, leaf inclination angle distribution and foliage and canopy spatial

712 clumping (Cescatti & Niinemets, 2004; Kobayashi *et al*., 2007; Chen *et al*., 2012; Disney, 2015;

713 Drewry *et al.* 2014; Wu *et al*. 2016a,b). Furthermore, due to gaps in the canopy, leaves at a

714 given value of cumulative leaf area index can be sunlit or shaded, further complicating the

715 estimation of light at the leaf surface, leaf absorption, and the subsequent numeric integration

716 of canopy-scale photosynthetic, water, and energy fluxes (de Pury & Farquhar, 1997; Wang &

717 Leuning, 1998; de Pury & Farquhar, 1999; Kobayashi *et al*., 2012). Here, the models differ in

718   how these scaling issues are addressed (Table 1) and based on how the canopy is considered,

719   they can be broadly divided between multi-layer models and big-leaf models.

720

721   Several TBMs have used the "big leaf" approach where a canopy approximately represents a

722   single big leaf with a single set of traits describing the photosynthetic capacity together with

723   characteristic light and temperature response functions (generally by PFT), typically scaled to

724   the canopy as a function of leaf area index (e.g., Amthor, 1994; Sands, 1996). Although

725   sometimes still used (e.g. G'DAY, Table 1), the big leaf model approach consisting of a single

726   "leaf" has been demonstrated to be prone to major integration errors due to lack of

727   consideration of sunlit and shaded leaf area classes (de Pury & Farquhar, 1997; Friend, 2001).

728   These errors were somewhat reduced by developing the "two big-leaf" model approach, which

729   consists of separate handling of a representative sunlit and a shaded big leaf (de Pury &

730   Farquhar, 1997; Chen et $al.$, 1999; Dai et $al.$, 2004). Indeed, separate integration of A for sunlit

731   and shaded leaf fractions provides a much more accurate integration of carbon and water

732   fluxes (de Pury & Farquhar, 1997; Dai et $al.$, 2004), and this is the approach used in several

733   contemporary TBMs (Table 1).

734

735   Big leaf models differ in how whole-canopy $V_{c,max}$ and J_{max} values are derived (or sunlit and

736   shaded big leaf values are derived), but typically, proportionality of photosynthetic capacity and

737   average light (deemed optimal) is assumed (Table 1, Amthor, 1994; Sands, 1995a; Sands,

738   1995b). Yet, such optimality is not present in nature (Niinemets, 2012). In fact, the decline of

739   photosynthetic capacity through the canopy is much shallower than that for light (Lloyd et $al.$,

740   2010; Dewar *et al*. 2012; Niinemets *et al*., 2015). Such departures from optimality have been

741   considered in some multi-layer models (Table 1), but nevertheless, only a few datasets have

742   been used to develop global parameterizations for multi-layer models (e.g., Carswell *et al*.,

743   2000; Lloyd *et al*., 2010). PFT and biome-dependent within-canopy acclimation patterns have

744   recently been highlighted (Niinemets *et al*., 2015) and could be used in future model

745   development.

746

747   Depending on the distribution of foliage inclination angles and spatial clumping, the probability

748   for light penetration varies at a given cumulative LAI (Cescatti & Niinemets, 2004; Disney,

749   2015). Importantly, characteristic canopy features differ among PFTs given fundamental

750   differences in leaf habit and growth forms (Cescatti & Niinemets, 2004), as a result of land-use,

751   landscape legacies and past disturbance, but few TBMs take this into account. While the multi-

752   layer models can be easily modified to incorporate different clumping and foliage inclination

753   angles, this is much less straightforward for the big leaf models. In fact, differences in canopy

754   architecture are part of the whole-canopy $V_{c,max}$ and J_{max} values in current big leaf models, i.e.

755   the input values get converted to canopy-scale sunlit and shaded values blurring the definition

756   of $V_{c,max}$ and J_{max} and making comparison with measured leaf level values impossible.

757   Moreover, leaf optical properties and foliar traits change markedly within the vertical canopy

758   profile (Serbin *et al*., 2014; Wu *et al*., 2016b; Yang *et al*., 2016), but are often assumed static,

759   which will generally lead to improper representation of light interception and utilization. This

760   improper representation will feed forward to the integration of leaf energy balance and carbon

761   uptake. We argue that traits like $V_{c,max}$ and J_{max} should retain their original physiological

762   definition and that more effort is needed to improve the representation of canopy

763   architecture and subsequent scaling of foliar properties in TBMs. Modifications to the

764   underlying radiative transfer model (RTM) structure and scaling can help to improve the

765   representation of the canopy light environment and modeling of carbon, water, and energy

766   fluxes (Kobayashi *et al*., 2012), however increasing RTM complexity or vertical layering should

767   not come at the cost of the ability to parameterize the model. A promising means to constrain

768   these approaches is through model-data integration whereby remote sensing observations (e.g.

769   optical, LiDAR) from the leaf to landscape are used to inform the RTM structure and to

770   parameterize across spatial and temporal scales (e.g. Shiklomanov *et al*. 2016).

771   *Recommendations: (17) TBMs should not use single layer big leaf models. (18) We need better*

772   *model representation of canopy architecture and vertical scaling of foliar properties, and data to*

773   *evaluate alternative radiative transfer models and scaling approaches.*

774

775   **Canopy to landscape scaling**

776

777   There is considerable variability in plant physiological traits across space and time (Serbin *et al*.,

778   2015; Singh *et al*., 2015), even within an individual species or PFT (Kattge *et al.* 2011; Serbin *et*

779   *al*., 2014). This variability is driven by differences across vegetation types, photosynthetic

780   pathways, plant successional status, as well as a result of nutrient availability and other abiotic

781   factors. There is a propensity for strong covariance among many key physiological traits as well

782   as fundamental tradeoffs which determine the distribution of these properties across

783   landscapes. Moreover, the nonlinearity in the scaling of model processes from leaf to larger

784   regions requires careful consideration of model parameterization in order to effectively capture

785   the larger-scale emergent responses (Fisher *et al.*, 2015). Parameterization with single, fixed

786   values of photosynthetic capacity likely obscures the true response of vegetation to global

787   change across landscapes, particularly at the current climatic extents of vegetation, thus

788   inadequately capturing critical plant threshold responses to factors such as temperature and

789   precipitation. The links between leaf-level observations, environmental responses and

790   emergent landscape-scale parameterizations needed for TBMs is are not straightforward, and

791   as such global parameterizations are commonly derived through the inversion of large-scale

792   datasets (e.g. Kattge *et al.*, 2009; Lin *et al.*, 2015). However use of such data sets can yield

793   parameterization that is inconsistent with current model structures resulting in unrealistic

794   model outputs (e.g. Bonan *et al.*, 2012). Furthermore, the trade-offs among variables (e.g.

795    $V_{c,max}$ v N) are themselves scale-dependent, with slopes changing depending on whether one is

796   looking at an across-PFT evolutionary constraint, a within-PFT community response, or a within-

797   individual phenotypic response (Feng and Dietze 2014). Care must be taken to not use data

798   constraints at one scale (e.g. global) to drive responses at another scale (e.g. responses to

799   change over time).

800

801   The increasing use of trait databases (Wright *et al.*, 2004; Kattge *et al.*, 2011) in modeling

802   activities has started to address some of these issues by leveraging more comprehensive

803   descriptions of traits within models and across PFTs (LeBauer *et al.*, 2013; Dietze *et al.*, 2014;

804   Fisher *et al.*, 2015). These databases should also be used to more extensively explore trait-

805   environment relationships. New, model-data integration frameworks (e.g. LeBauer *et al.*, 2013;

806   Dietze *et al*., 2014) can be used to explore the capacity to adequately parameterize existing and

807   new model representations, expand PFT descriptions, as well as identify critical model

808   uncertainties and data gaps and thus prioritize observational and model development activities

809   (Dietze *et al*., 2014). Given the current diverse methods used to parameterize photosynthetic

810   parameters (Rogers, 2014), the available data (e.g. Kattge *et al*. 2011), and new opportunities

811   to markedly expand databases (e.g. Serbin *et al* 2012, De Kauwe *et al.* 2016), we recommend

812   that models should now use common parameterizations for photosynthetic parameters e.g.

813    $V_{c,max}$ and J_{max} that are constrained by the available data and consistent with known trait

814   covariance, thereby removing unnecessary uncertainty from model projections.

815

816   The capacity to utilize remote sensing observations to inform model parameterizations,

817   representations, and trait-environment relationships across spatial and temporal scales is

818   increasing (Dahlin *et al*., 2013; Serbin *et al*., 2015; Schimel *et al*., 2015; Shugart *et al*., 2015;

819   Singh *et al*., 2015). Importantly, remote sensing observations can provide a synoptic view of

820   trait variability and functional diversity across landscapes (e.g. Dahlin *et al*., 2013; Asner *et al*.

821   2015; Singh *et al*., 2015) and identify emergent relationships that could be included in next-

822   generation trait-based models. These observations can also be used as important datasets to

823   benchmark prognostic traits at the relevant spatial scales (e.g. Fisher *et al*., 2015). Proposed

824   and upcoming and satellite missions, including NASA's Hyperspectral Infrared Imager (HyspIRI)

825   mission concept (Lee *et al*., 2015) and the European Space Agencies Environmental Mapping

826   and Analysis Program (EnMAP; Guanter *et al*., 2015), will provide a critical capacity to provide

827   this information for global-scale models.

828   *Recommendations: (19) Data constraints (e.g. trait tradeoffs) must be applied at the relevant*

829   *spatial and temporal scales. (20) Where possible, TBMs should use common parameterization*

830   *for photosynthetic parameters. (21) TBMs should make better use of remote sensing data to*

831   *inform model parameterizations and test predictions.*

832

833   **Conclusion**

834

835   Realistic model representation of A, and more broadly, plant physiological processes, should be

836   an essential component of TBMs because that same plant physiology is determining the

837   response of the terrestrial biosphere to global change, including the fate of the terrestrial

838   carbon sink. However, many TBMs fail to accurately represent photosynthetic responses to key

839   environmental variables. Here, in a subset of TBMs, we have shown marked model divergence

840   in the representation of key physiological responses for a single well-defined PFT. We have

841   made 21 recommendations that highlight where steps can be taken to improve existing model

842   representation. Our recommendations include areas where immediate steps could be taken,

843   areas where model development is hindered by a lack of physiological data and several

844   important avenues of research that are critical to our understanding that are not currently

845   mature enough to include in model structures. These recommendations are summarized in Fig.

846   6.

847   Current model representation of A has a foundation in research conducted in temperate

848   climates. However, other biomes that are climatically sensitive and globally important are

849   understudied, and therefore process representation in these biomes is uncertain; the Arctic and

850   tropics deserve particular attention. The approach taken here, i.e. evaluating how TBMs

851   reproduce physiological responses to key environmental drivers, was found to be extremely

852   informative by all who participated. We feel the process provides a useful template for

853   meaningful collaboration between empiricists and modelers and that including the

854   physiological outputs considered here as readily available diagnostic features would be a highly

855   valuable feature to include in new TBMs. This study also highlighted the need for a multi-

856   assumption model framework within which the modeling community and domain experts could

857   evaluate different model structures and parameterization approaches and quantitatively

858   evaluate their effect on model outputs. Such a framework would provide a forum where

859   modelers and, in this case, physiologists could reach agreement over the best approaches for

860   representing and parameterizing the sub-processes within complex TBMs.

861

862   **Acknowledgements**

863

872 **References**

873

874 **Ainsworth EA, Long SP. 2005.** What have we learned from 15 years of free-air CO_2 enrichment

875 (FACE)? A meta-analytic review of the responses of photosynthesis, canopy properties and

876 plant production to rising CO_2. *New Phytologist* **165**: 351-371.

877

878 **Ainsworth EA, Rogers A. 2007.** The response of photosynthesis and stomatal conductance to

879 rising CO_2: mechanisms and environmental interactions. *Plant Cell & Environment,* **30**: 258-270.

880

881 **Ainsworth EA, Rogers A, Nelson R, Long SP. 2004.** Testing the "source-sink" hypothesis of

882 down-regulation of photosynthesis in elevated CO_2 in the field with single gene substitutions in

883 Glycine max. *Agricultural and Forest Meteorology* **122**: 85-94.

884

885 **Ali AA, Xu CG, Rogers A, McDowell NG, Medlyn BE, Fisher RA, Wullschleger SD, Reich PB,**

886 **Vrugt JA, Bauerle WL, et al. 2015.** Global-scale environmental control of plant photosynthetic

887 capacity. *Ecological Applications* **25:** 2349-2365.

888

889 **Amthor JS. 1994.** Scaling CO_2-photosynthesis relationships from the leaf to the canopy.

890 *Photosynthesis Research* **39:** 321-350.

891

892 **Aphalo PJ, Jarvis PG. 1991.** Do stomata respond to relative-humidity. *Plant Cell & Environment*

893 **14**: 127-132.

894

895 **Arneth A, Mercado L, Kattge J, Booth B. 2012.** Future challenges of representing land-

896 processes in studies on land-atmosphere interactions. *Biogeosciences* **9**:3587-3599.

897

898 **Asner GP, Martin RE, Anderson CB, Knapp DE. 2015.** Quantifying forest canopy traits: Imaging

899 spectroscopy versus field survey. *Remote Sensing of Environment* **158:** 15-27.

900

901 **Atkin OK, Tjoelker MG. 2003.** Thermal acclimation and the dynamic response of plant

902 respiration to temperature. *Trends in Plant Science* **8**: 343-351.

903

904 **Atkin OK, Bloomfield KJ, Reich PB, Tjoelker MG, Asner GP, Bonal D, Bonisch G, Bradford M,**

905 **Cernusak LA, Cosio EG *et al*. 2015.** Global variability in leaf respiration in relation to climate,

906 plant functional types and leaf traits. *New Phytologist* **206:** 614-636.

907

908 **Ball TJ, Woodrow IE, Berry JA. 1987.** A model predicting stomatal conductance and its

909 contribution to the control of photosynthesis under different environmental conditions. *In* I.

910 Biggins (ed.) progress in photosynthesis research. Martinus Nijhoff Publishers, the Netherlands.

911 pp 221-224.

912

913 **Bauerle WL, Oren R, Way DA, Qian SS, Stoy PC, Thornton PE, Bowden JD, Hoffman FM,**

914 **Reynolds RF. 2012.** Photoperiodic regulation of the seasonal pattern of photosynthetic capacity

915 and the implications for carbon cycling. *Proceedings of the National Academy of Sciences of the*

916 *United States of America* **109:** 8612-8617.

917

918 **Bauerle WL, Daniels AB, Barnard DM. 2014.** Carbon and water flux responses to physiology by

919 environment interactions: a sensitivity analysis of variation in climate on photosynthetic and

920 stomatal parameters. *Climate Dynamics* **42**: 2539-2554.

921

922 **Beer C, Reichstein M, Tomelleri E, Ciais P, Jung M, Carvalhais N, Rodenbeck C, Arain MA,**

923 **Baldocchi D, Bonan GB,** *et al*. **2010.** Terrestrial Gross Carbon Dioxide Uptake: Global

924 Distribution and Covariation with Climate. *Science,* **329**: 834-838.

925

926 **Bernacchi CJ, Singsaas EL, Pimentel C, Portis Jr AR, Long SP. 2001.** Improved temperature

927 response functions for models of Rubisco-limited photosynthesis. *Plant, Cell & Environment*, **24**:

928 253-259.

929

930 **Bernacchi CJ, Calfapietra C, Davey PA, Wittig VE, Scarascia-Mugnozza GE, Raines CA, Long SP.**

931 **2003.** Photosynthesis and stomatal conductance responses of poplars to free-air CO_2

932 enrichment (PopFACE) during the first growth cycle and immediately following coppice. *New*

933 *Phytologist* **159:** 609-621.

934

935 **Berry JA, Björkman O. 1980.** Photosynthetic response and adaptation to temperature in higher-

936 plants. *Annual Review of Plant Physiology and Plant Molecular Biology* **31:** 491-543.

937

Best MJ, Pryor M, Clark DB, Rooney GG, Essery RLH, Menard CB, Edwards JM, Hendry MA

Porson A, Gedney N *et al*. **2011.** The Joint UK Land Environment Simulator (JULES), model

description – Part 1: Energy and water fluxes. *Geoscientific Model Development* **4:** 677-699.

941

Bjorkman O, Badger M. 1979. Time course of thermal acclimation of the photosynthetic

apparatus in Nerium oleander. *Carnegie Inst. Washington Yearb.* **78:** 262-75

944

Boden TA, Marland G, Andres RJ. 2013. Global, regional and national fossil-fuel CO_2 emissions.,

Oak Ridge, Carbon Dioxide Information Analysis Center, Oak Ridge National Laboratory, U.S.

Department of Energy.

948

Bonan GB, Lawrence PJ, Oleson KW, Levis S, Jung M, Reichstein M, Lawrence DM, Swenson

SC. 2011. Improving canopy processes in the Community Land Model version 4 (CLM4) using

global flux fields empirically inferred from FLUXNET data. *Journal of Geophysical Research* **116:**

G02014

953

Bonan GB, Oleson KW, Fisher RA, Lasslop G, Reichstein M. 2012. Reconciling leaf physiological

traits and canopy flux data: Use of the TRY and FLUXNET databases in the Community Land

Model version 4. *Journal of Geophysical Research-Biogeosciences* **117**, G02026

957

958 **Bonan GB, Williams M, Fisher RA, Oleson KW. 2014.** Modeling stomatal conductance in the

959 earth system: linking leaf water-use efficiency and water transport along the soil-plant-

960 atmosphere continuum. *Geoscientific Model Development* **7**, 2193-2222.

961

962 **Bunce JA. 2000.** Responses of stomatal conductance to light, humidity and temperature in

963 winter wheat and barley grown at three concentrations of carbon dioxide in the field. *Global*

964 *Change Biology* **6:** 371-382

965

966 **Busch F. 2013.** Current methods for estimating the rate of photorespiration in leaves. *Plant*

967 *Biology* **15:** 648-655.

968

969 **Busch F, Hüner NPA, Ensminger I. 2007.** Increased air temperature during simulated autumn

970 conditions does not increase photosynthetic carbon gain but affects the dissipation of excess

971 energy in seedlings of the evergreen conifer Jack pine. *Plant Physiology* **143:** 1242-1251.

972

973 **Campbell C, Atkinson L, Zaragoza-Castells J, Lundmark M, Atkin O, Hurry V. 2007.** Acclimation

974 of photosynthesis and respiration is asynchronous in response to changes in temperature

975 regardless of plant functional type. *New Phytologist* **176:** 375–389.

976

977 **Carswell FE, Meir P, Wandelli EV, Bonates LCM, Kruijt B, Barbosa EM, Nobre AD, Grace J,**

978 **Jarvis PG. 2000.** Photosynthetic capacity in a central Amazonian rain forest. *Tree Physiology* **20:**

979 179-186.

980

Cescatti A, Niinemets Ü 2004. Sunlight capture. Leaf to landscape. In: Smith WK, Vogelmann

TC, Chritchley C eds. Photosynthetic adaptation. Chloroplast to landscape. Berlin: Springer

Verlag, 42-85.

984

Chaves MM, Flexas J, Pinheiro C. 2009. Photosynthesis under drought and salt stress:

regulation mechanisms from whole plant to cell. *Annals of Botany*, **103:** 551-560.

987

Chen JM, Liu J, Cihlar J, Goulden ML. 1999. Daily Canopy Photosynthesis Model Through

Temporal and Spatial Scaling for Remote Sensing Applications. *Ecological Modelling* **124:** 99-

119.

991

Chen JM, Mo G, Pisek J, Liu J, Deng F, Ishizawa M, Chan D. 2012. Effects of foliage clumping on

the estimation of global terrestrial gross primary productivity. *Global Biogeochemical Cycles* **26**,

GB1019.

995

Christmann A, Weiler EW, Steudle E, Grill E. 2007. A hydraulic signal in root-to-shoot signalling

of water shortage. *Plant Journal* **52:** 167-174.

998

**Ciais P, Gasser T, Paris JD, Caldeira K, Raupach MR, Canadell JG, Patwardhan A, Friedlingstein

P, Piao SL *et al*. 2013.** Attributing the increase in atmospheric CO_2 to emitters and absorbers.

Nature Climate Change **3:** 926-930.

1002

1003 **Collatz GJ, Ball JT, Grivet C, Berry JA (1991**) Physiological and environmental regulation of

1004 stomatal conductance, photosynthesis and transpiration – a model that includes laminar

1005 boundary layer. *Agricultural and Forest Meteorology* **54:** 107-136.

1006

1007 **Clark DB, Mercado LM, Sitch S, Jones CD, Gedney N, Best MJ, Pryor M, Rooney GG, Essery**

1008 **RLH, Blyth E *et al*. 2011.** The Joint UK Land Environment Simulator (JULES), model description –

1009 Part 2: Carbon fluxes and vegetation dynamics. *Geoscientific Model Development* **4:** 701-722.

1010

1011 **Cowan IR, Farquhar GD. 1977.** Stomatal function in relation to leaf metabolism and

1012 environment. In: Integration of Activity in the Higher Plant (ed. Jennings DH), pp. 471–505.

1013 Cambridge University Press, Cambridge.

1014

1015 **Crafts-Brandner SJ, van de Loo FJ, Salvucci ME. 1997.** The two forms of ribulose-1,5-

1016 bisphosphate carboxylase/oxygenase activase differ in sensitivity to elevated temperature.

1017 *Plant Physiology*, 114, 439-444.

1018

1019 **Cramer W, Bondeau A, Woodward FI, Prentice IC, Betts RA, Brovkin V, Cox PM, Fisher V, Foley**

1020 **JA, Friend AD *et al*. 2001.** Global response of terrestrial ecosystem structure and function to

1021 CO_2 and climate change: results from six dynamic global vegetation models. *Global Change*

1022 *Biology* **7**: 357-373.

1023

1024 **Dai Y-J, Dickinson RE, Wang YP. 2004.** A two-big-leaf model for canopy temperature,

1025 photosynthesis, and stomatal conductance. *Journal of Climate* **17:** 2281-2299.

1026

1027 **Dahlin KM, Asner GP, Field CB. 2013.** Environmental and community controls on plant canopy

1028 chemistry in a Mediterranean-type ecosystem. *Proceedings of the National Academy of*

1029 *Sciences* **110:** 6895-6900.

1030

1031 **Drewry DT, Kumar P, Long SP. 2014.** Simultaneous improvement in productivity, water use, and

1032 albedo through crop structural modification. *Global Change Biology* **20**: 1955-1967.

1033

1034 **de Pury DGG, Farquhar GD. 1997.** Simple scaling of photosynthesis from leaves to canopies

1035 without the errors of big-leaf models. *Plant, Cell & Environment* **20:** 537-557.

1036

1037 **de Pury DGG, Farquhar GD. 1999.** A commentary on the use of a sun/shade model to scale

1038 from the leaf to a canopy. *Agricultural and Forest Meteorology* **95:** 257-260.

1039

1040 **De Beeck MO, Gielen B, Jonckheere I, Samson R, Janssens IA, Ceulemans R. 2010.** Needle age-

1041 related and seasonal photosynthetic capacity variation is negligible for modelling yearly gas

1042 exchange of a sparse temperate Scots pine forest. *Biogeosciences,* **7**: 199-215.

1043

1044 **De Kauwe MG, Medlyn BE, Zaehle S Walker AP, Dietze MC, Hickler T, Jain AK, Luo YQ, Parton**

1045 **WJ, Prentice IC. 2013.** Forest water use and water use efficiency at elevated CO2: a model-data

1046   intercomparison at two contrasting temperate forest FACE sites. *Global Change Biology* **19**,

1047   1759-1779.

1048

1049   **De Kauwe MG, Zhou SX, Medlyn BE, Pitman AJ, Wang YP, Duursma RA, Prentice IC. 2015.** Do

1050   land surface models need to include differential plant species responses to drought? Examining

1051   model predictions across a mesic-xeric gradient in Europe. *Biogeosciences* **12**, 7503-7518.

1052

1053   **De Kauwe MG, Lin YS, Wright IJ, Medlyn BE, Crous KY, Ellsworth DS, Maire V, Prentice IC,**

1054   **Atkin OK, Rogers A** *et al*. **2016.** A test of the 'one-point method' for estimating maximum

1055   carboxylation capacity from field-measured, light-saturated photosynthesis. *New Phytologist*

1056   **210:** 1130-1144.

1057

1058   **Dewar RC. 2002.** The Ball-Berry-Leuning and Tardieu-Davies stomatal models: synthesis and

1059   extension within a spatially aggregated picture of guard cell function. *Plant Cell & Environment*

1060   **25:** 1383-1398.

1061

1062   **Dewar RC, Tarvainen L, Parker K, Wallin G, Mcmurtrie RE. 2012.** Why does leaf nitrogen

1063   decline within tree canopies less rapidly than light? An explanation from optimization subject to

1064   a lower bound on leaf mass per area. *Tree Physiology* **32**, 520-534.

1065

1066   **Dietze MC. 2014.** Gaps in knowledge and data driving uncertainty in models of photosynthesis.

1067   *Photosynthesis Research* **119**: 3-14.

1068

Disney M. 2015. Remote sensing of vegetation: potentials, limitations, developments and applications. In: Hikosaka K, Anten NPR, Niinemets Ü eds. Canopy photosynthesis: from basics to applications. Berlin: Springer Verlag, pp289-331.

1072

Doughty CE, Goulden ML. 2008. Seasonal patterns of tropical forest leaf area index and CO_2 exchange. *Journal of Geophysical Research: Biogeosciences* **113**: G00B07

1075

Egea G, Verhoef A, Vidale PL. 2011. Towards an improved and more flexible representation of water stress in coupled photosynthesis-stomatal conductance models. *Agricultural and Forest Meteorology* **151**: 1370-1384.

1079

Ethier GJ, Livingston NJ. 2004. On the need to incorporate sensitivity to CO_2 transfer conductance into the Farquhar-von Caemmerer-Berry leaf photosynthesis model. *Plant, Cell & Environment* **27:** 137-153.

1083

Farquhar GD, von Caemmerer S. Berry JA. 1980. A biochemical-model of photosynthetic CO_2 assimilation in leaves of C_3 species. *Planta* **149**: 78-90.

1086

Feng X, Dietze M. 2013. Scale dependence in the effects of leaf ecophysiological traits on photosynthesis: Bayesian parameterization of photosynthesis models. *New Phytologist* **200:** 1132-1144.

1090

1091   **Fisher JB, Badgley G, Blyth E. 2012.** Global nutrient limitation in terrestrial vegetation. *Global*

1092   *Biogeochemical Cycles* **26:** GB3007.

1093

1094   **Fisher JB, Huntzinger DN, Schwalm CR, Sitch S. 2014.** Modeling the Terrestrial Biosphere.

1095   *Annual Review of Environment and Resources* **39:** 91-123.

1096

1097   **Fisher RA, Muszala S, Verteinstein M, Lawrence P, Xu C, McDowell NG, Knox RG, Koven CD,**

1098   **Holm J, Rogers BM *et al*. 2015.** Taking off the training wheels: the properties of a dynamic

1099   vegetation model without climate envelopes, CLM4.5(ED). *Geoscientific Model Development* **8:**

1100   3593-3619.

1101

1102   **Flexas J, Barbour MM, Brendel O, Cabrera HM, Carriqui M, Diaz-Espejo A, Douthe C, Dreyer E,**

1103   **Ferrio JP, Gago J, *et al*. 2012.** Mesophyll diffusion conductance to CO_2: An unappreciated

1104   central player in photosynthesis. *Plant Science* **193**: 70-84.

1105

1106   **Foley JA, Prentice IC, Ramankutty N, Levis S, Pollard D, Sitch S, Haxeltine A. 1996.** An

1107   integrated biosphere model of land surface processes, terrestrial carbon balance, and

1108   vegetation dynamics. *Global Biogeochemical Cycles* **10:** 603-628.

1109

1110   **Friend AD. 2010.** Terrestrial plant production and climate change. *Journal of Experimental*

1111   *Botany* **61:** 1293-1309.

1112

1113 **Friedlingstein P, Cox P, Betts R, Bopp L, von Bloh W, Brovkin V, Cadule P, Doney S Eby M, Fung**

1114 **I** *et al.* **2006.** Climate-carbon cycle feedback analysis: Results from the (CMIP)-M-4 model

1115 intercomparison. *Journal of Climate* **19**: 3337-3353.

1116

1117 **Friedlingstein P, Meinshausen M, Arora VK, Jones CD, Anav A, Liddicoat SK, Knutti R. 2014.**

1118 Uncertainties in CMIP5 Climate Projections due to Carbon Cycle Feedbacks. *Journal of Climate*

1119 **27:** 511-526.

1120

1121 **Friend AD. 2001.** Modelling canopy CO2 fluxes: are 'big-leaf' simplifications justified? *Global*

1122 *Ecology and Biogeography* **10:** 603-619.

1123

1124 **Galmés J, Kapralov MV, Copolovici LO, Hermida-Carrera C, Niinemets Ü. 2015.** Temperature

1125 responses of the Rubisco maximum carboxylase activity across domains of life: phylogenetic

1126 signals, trade-offs, and importance for carbon gain. *Photosynthesis Research* **123**: 183-201.

1127

1128 **Gregory JM, Jones CD, Cadule P, Friedlingstein P. 2009.** Quantifying Carbon Cycle Feedbacks.

1129 *Journal of Climate* **22**: 5232-5250.

1130

1131 **Gu LH, Baldocchi D, Verma SB, Black TA, Vesala T, Falge EM, Dowty PR. 2002.** Advantages of

1132 diffuse radiation for terrestrial ecosystem productivity. *Journal of Geophysical Research-*

1133 *Atmospheres* **107**: 4050.

1134

1135   **Guanter L, Kaufmann H, Segl K, Foerster S, Rogass C, Chabrillat S, Kuester T, Hollstein A,**

1136   **Rossner G, Chlebek C, *et al*. 2015.** The EnMAP Spaceborne Imaging Spectroscopy Mission for

1137   Earth Observation. *Remote Sensing* **7:** 8830.

1138

1139   **Gunderson CA, O'Hara KH, Campion CM, Walker AV, Edwards NT. 2010.** Thermal plasticity of

1140   photosynthesis: the role of acclimation in forest responses to a warming climate. *Global Change*

1141   *Biology* **16:** 2272-2286.

1142

1143   **Hannemann J, Poorter H, Usadel B, Blasing OE, Finck A, Tardieu F, Atkin OK, Pons T, Stitt M,**

1144   **Gibon Y. 2009.** Xeml Lab: a tool that supports the design of experiments at a graphical interface

1145   and generates computer-readable metadata files, which capture information about genotypes,

1146   growth conditions, environmental perturbations and sampling strategy. *Plant Cell &*

1147   *Environment* **32**: 1185-1200.

1148

1149   **Hari P, Makela A, Korpilahti E, Holmberg M. 1986.** Optimal control of gas exchange. *Tree*

1150   *Physiology* **2**: 169-175.

1151 **Harper A, Cox P, Friedlingstein P, Wiltshire A, Jones C, Sitch S, Mercado LM, Roberston E,**

1152 **Kattge J, *et al*. 2016.** Improved representation of plant functional types and physiology in the

1153 Joint UK Land Environment Simulator (JULES v4.2) using plant trait information. *Geoscientific*

1154 *Model Development*. doi:10.5194/gmd-2016-22.

1155

1156 **Huntingford C, Smith DM, Davies WJ, Falk R, Sitch S, Mercado LM. 2015.** Combining the [ABA]

1157 and net photosynthesis-based model equations of stomatal conductance. *Ecological modelling*

1158 **300:** 81–88.

1159

1160 **IPCC. 2013.** Climate Change 2013: The Physical Science Basis. Contribution of Working Group I

1161 to the Fifth Assessment Report of the Intergovernmental Panel on Climate Change. (eds

1162 Stocker TF, Qin D, Plattner G-K, Tignor M, Allen SK, Boschung J, Nauels A, Xia Y, Bex V, Midgley

1163 PM) pp 1535, Cambridge University Press, Cambridge, United Kingdom and New York, NY, USA.

1164

1165 **Jacobs CMJ. 1994.** Direct impact of atmospheric CO_2 enrichment on regional transpiration. PhD

1166 thesis, Wageningen Agricultural University, Wageningen, the Netherlands, ISBN 90-5485-250-X,

1167

1168 **Jarvis PG. 1995.** Scaling processes and problems. *Plant, Cell & Environment* **18:** 1079-1089.

1169

1170 **Jones AM. 2016.** A new look at stress: abscisic acid patterns and dynamics at high-resolution.

1171 Tansley insight. *New Phytologist* **210:** 38-44

1172

1173 **Jordan DB, Ogren WL. 1984.** The CO_2/O_2 specificity of ribulose 1,5-bisphosphate

1174 carboxylase/oxygenase. Dependence on ribulose bisphosphate concentration, pH and

1175 temperature. *Planta* **161**: 308-313.

1176

1177 **June T, Evans JR, Farquhar GD. 2004.** A simple new equation for the reversible temperature

1178 dependence of photosynthetic electron transport: a study on soybean leaf. *Functional Plant*

1179 *Biology* **31:** 275-283

1180

1181 **Kattge J, Knorr W. 2007.** Temperature acclimation in a biochemical model of photosynthesis: a

1182 reanalysis of data from 36 species. *Plant Cell and Environment* **30**: 1176-1190.

1183

1184 **Kattge J, Knorr W, Raddatz TJ, Wirth C. 2009.** Quantifying photosynthetic capacity and its

1185 relationship to leaf nitrogen content for global-scale terrestrial biosphere models. *Global*

1186 *Change Biology* **15:** 976-991.

1187

1188 **Kattge J, Diaz S, Lavorel S *et al.* 2011.** TRY - a global database of plant traits. *Global Change*

1189 *Biology,* **17**, 2905-2935.

1190

1191 **Katul G, Manzoni S, Palmroth S, Oren R. 2010.** A stomatal optimization theory to describe the

1192 effects of atmospheric CO2 on leaf photosynthesis and transpiration. *Annals of Botany* **105**,

1193 431-442.

1194

1195   **Keenan T, Sabate S, Gracia C. 2010.** The importance of mesophyll conductance in regulating

1196   forest ecosystem productivity during drought periods. *Global Change Biology* **16**: 1019-1034.

1197

1198   **Kelly JWG, Duursma RA, Atwell BA, Tissue DT, Medlyn BE. 2015.** Drought x CO_2 interactions in

1199   trees: a test of the low-C_i mechanism. *New Phytologist* **209:** 1600-1612

1200

1201   **Knorr W, Heimann M. 2001.** Uncertainties in global terrestrial biosphere modeling 1. A

1202   comprehensive sensitivity analysis with a new photosynthesis and energy balance scheme.

1203   *Global Biogeochemical Cycles* **15:** 207-225.

1204

1205   **Kobayashi H, Suzuki R, Kobayashi S. 2007.** Reflectance seasonality and its relation to the

1206   canopy leaf area index in an eastern Siberian larch forest: Multi-satellite data and radiative

1207   transfer analyses. *Remote Sensing of Environment* **106**: 238-252.

1208

1209   **Kobayashi H, Baldocchi DD, Ryu Y, Chen Q, Ma S, Osuna JL, Ustin SL. 2012.** Modeling energy

1210   and carbon fluxes in a heterogeneous oak woodland: A three-dimensional approach.

1211   *Agricultural and Forest Meteorology* **152**: 83-100.

1212

1213   **Kull O, Kruijt B. 1998.** Leaf photosynthetic light response: a mechanistic model for scaling

1214   photosynthesis to leaves and canopies. *Functional Ecology* **12**: 767-777.

1215

1216 **Leakey ADB, Ainsworth EA, Bernacchi CJ, Rogers A, Long SP, Ort DR. 2009.** Elevated CO_2

1217 effects on plant carbon, nitrogen, and water relations: six important lessons from FACE. *Journal*

1218 *of Experimental Botany* **60**: 2859-2876.

1219

1220 **Lebauer DS, Wang D, Richter KT, Davidson CC, Dietze MC. 2013.** Facilitating feedbacks

1221 between field measurements and ecosystem models. *Ecological Monographs* **83:** 133-154.

1222

1223 **Lee CM, Cable ML, Hook SJ, Green RO, Ustin SL, Mandl DJ, Middleton EM. 2015.** An

1224 introduction to the NASA Hyperspectral InfraRed Imager (HyspIRI) mission and preparatory

1225 activities. *Remote Sensing of Environment* **167:** 6-19.

1226

1227 **Le Quéré C, Moriarty R, Andrew R *et al.* 2015.** Global Carbon Budget 2015. *Earth System*

1228 *Science Data Discussions,* **7**: 349-396.

1229

1230 **Leuning R. 1995.** A critical appraisal of a combined stomatal-photosynthesis model for C3

1231 plants. *Plant Cell & Environment*, **18:** 339-355.

1232

1233 **Leuning R, Tuzet A, Perrier A. 2004.** Stomata as part of the soil-plant-atmosphere continuum.

1234 In: Forests at the Land-Atmosphere Interface (eds M. Mencuccini, J. Grace, J. Moncrieff and K.G.

1235 McNaughton) CAB International, Oxford. pp 9 - 28.

1236

1237   **Lin YS, Medlyn BE, Ellsworth DS. 2012.** Temperature responses of leaf net photosynthesis: the

1238   role of component processes. *Tree Physiology* **32:** 219-231

1239

1240   **Lin YS, Medlyn BE, DeKauwe MG, Ellsworth DS. 2013.** Biochemical photosynthetic responses to

1241   temperature: how do interspecific differences compare with seasonal shifts? *Tree Physiology*

1242   **33:** 793-806

1243

1244   **Lin YS, Medlyn BE, Duursma RA Prentice IC, Wang H, Baig S, Eamus D, Resco de Dios V,**

1245   **Mitchell P Ellsworth DS *et al.* 2015.** Optimal stomatal behaviour around the world. *Nature*

1246   *Climate Change* **5:** 459-464.

1247

1248   **Lloyd J, Patiño S, Paiva RQ, Nardoto GB, Quesada CA, Santos AJB, Baker TR, Brand WA, Hilke I,**

1249   **Gielmann H, *et al*. 2010.** Optimisation of photosynthetic carbon gain and within-canopy

1250   gradients of associated foliar traits for Amazon forest trees. *Biogeosciences* **7:** 1833-1859.

1251

1252   **Lobell DB, Roberts MJ, Schlenker W, Braun N, Little BB, Rejesus RM, Hammer GL. 2014.**

1253   Greater Sensitivity to Drought Accompanies Maize Yield Increase in the US Midwest. *Science*

1254   **344**, 516-519.

1255

1256   **Lombardozzi D, Bonan G, Smith NG, Dukes JS, Fisher R. 2015.** Temperature acclimation of

1257   photosynthesis and respiration: a key uncertainty in the carbon cycle-climate feedback.

1258   *Geophysical Research Letters* **42**: 8624-8631.

1259

Long SP. 1991. Modification of the response of photosynthetic productivity to rising

temperature by atmospheric CO_2 concentration - has its importance been underestimated.

Plant Cell & Environment **14**, 729-739.

1263

Long SP, Drake B. 1991. Effect of the long-term elevation of CO_2 concentration in the field on

the quantum yield of photosynthesis of the C3 sedge, *Scirpus olneyi*. *Plant Physiology* **96**: 221-

226.

1267

Long SP, Postl WF, Bolhar-Nordenkampf HR. 1993. Quantum yields for uptake of carbon

dioxide in C3 vascular plants of contrasting habitats and taxonomic groupings. *Planta* **189:** 226-

234.

1271

Long SP, Ainsworth EA, Rogers A, Ort DR. 2004. Rising atmospheric carbon dioxide: plants face

the future. *Annual Review of Plant Biology* **55:** 591-628.

1274

Lu ZM, Quinones MA, Zeiger E. 2000. Temperature dependence of guard cell respiration and

stomatal conductance co-segregate in an F_2 population of Pima cotton. *Australian Journal of*

Plant Physiology **27:** 457-462

1278

1279 **Luo Y, Su B, Currie WS, Dukes JS, Finzi AF, Hartwig U, Hungate B, McMurtrie RE, Oren R,**

1280 **Parton WJ *et al.* 2004.** Progressive nitrogen limitation of ecosystem responses to rising

1281 atmospheric carbon dioxide. *Bioscience* **54:** 731-739.

1282

1283 **Medlyn BE, Berbigier P, Clement R, Grelle A, Loustau D, Linder S, Wingate L, Jarvis PG,**

1284 **Sigurdsson BD, McMurtrie RE. 2005.** Carbon balance of coniferous forests growing in

1285 contrasting climates: Model-based analysis. *Agricultural and Forest Meteorology* **131:** 97-124.

1286

1287 **Medlyn BE, Dreyer E, Ellsworth DS, Forstreuter M, Harley PC, Kirschbaum MUF, Le Roux X,**

1288 **Montpied P, Strassemeyer J, Walcroft A, *et al*. 2002a.** Temperature response of parameters of

1289 a biochemically based model of photosynthesis. II. A review of experimental data. *Plant, Cell &*

1290 *Environment* **25**: 1167-1179.

1291

1292 **Medlyn BE, Loustau D, Delzon S. 2002b.** Temperature response of parameters of a

1293 biochemically based model of photosynthesis. I. Seasonal changes in mature maritime pine

1294 (Pinus pinaster Ait.). *Plant, Cell & Environment* **25:** 1155-1165

1295

1296 **Medlyn BE, Pepper DA, O'Grady AP, Keith H. 2007.** Linking leaf and tree water use with an

1297 individual-tree model. *Tree Physiology* **27**: 1687-1699

1298

1299   **Medlyn BE, Duursma RA, Eamus D, Ellsworth DS, Prentice IC, Barton CVM, Crous KY, De**

1300   **Angelis P, Freeman M, Wingate L. 2011.** Reconciling the optimal and empirical approaches to

1301   modelling stomatal conductance. *Global Change Biology,* **17**, 2134-2144.

1302

1303   **Medlyn BE, De Kauwe MG, Zaehle S, Walker AP, Duursma RA, Luus K, Mishurov M, Pak B,**

1304   **Smith B, Wang YPP, *et al*. 2016.** Using models to guide field experiments: *a priori* predictions

1305   for the CO_2 response of a nutrient- and water- limited native Eucalypt woodland. *Global*

1306   *Change Biology* **8:** 2834-2851.

1307

1308   **Medvigy D, Wofsy SC, Munger JW, Hollinger DY, Moorcroft PR. 2009.** Mechanistic scaling of

1309   ecosystem function and dynamics in space and time: Ecosystem Demography model version 2.

1310   *Journal of Geophysical Research-Biogeosciences* **114**. GO1002.

1311

1312   **Medvigy D. Jeong S-J, Clark KL, Skowronski NS, Schäfer KVR. 2013.** Effects of seasonal variation

1313   of photosynthetic capacity on the carbon fluxes of a temperate deciduous forest. *Journal of*

1314   *Geophysical Research* **118:** 1703-1714.

1315

1316   **Meir P, Mencuccini M, Dewar RC. 2015.** Drought-related tree mortality: addressing the gaps in

1317   understanding and prediction. *New Phytologist* **207:** 28-33.

1318

1319   **Mercado LM, Bellouin N, Sitch S, Boucher O, Huntingford C, Wild M, Cox, PM. 2009.** Impact of

1320   changes in diffuse radiation on the global land carbon sink. *Nature* **458:** 1014-1017.

1321

Moorcroft PR, Hurtt GC, Pacala SW. 2001. A method for scaling vegetation dynamics: The

ecosystem demography model (ED). *Ecological Monographs* **71:** 557-585.

1324

Mott KA. 2009. Opinion: Stomatal responses to light and CO_2 depend on the mesophyll. *Plant

Cell & Environment* **32:** 1479-1486.

1327

Niinemets U, Diaz-Espejo A, Flexas J, Galmes J. Warren CR. 2009. Importance of mesophyll

diffusion conductance in estimation of plant photosynthesis in the field. *Journal of Experimental

Botany* **60**: 2271-2282.

1331

Niinemets U, Keenan T. 2014. Photosynthetic responses to stress in Mediterranean evergreens:

Mechanisms and models. *Environmental and Experimental Botany* **103**: 24-41.

1334

Niinemets U, Tenhunen JD, Beyschlag W. 2004. Spatial and age-dependent modifications of

photosynthetic capacity in four Mediterranean oak species. *Functional Plant Biology* **31**: 1179-

1193.

1338

Niinemets Ü. 2012. Optimization of foliage photosynthetic capacity in tree canopies: towards

identifying missing constraints. *Tree Physiology* **32:** 505-509.

1341

1342 **Niinemets Ü, Anten NPR 2009.** Packing the photosynthesis machinery: from leaf to canopy. In:

1343 Laisk A, Nedbal L, Govindjee eds. Photosynthesis in silico: understanding complexity from

1344 molecules to ecosystems. Berlin: Springer Verlag, 363-399.

1345

1346 **Niinemets Ü, Keenan TF, Hallik L. 2015.** Tansley review. A worldwide analysis of within-canopy

1347 variations in leaf structural, chemical and physiological traits across plant functional types. *New*

1348 *Phytologist* **205:** 973-993.

1349

1350 **Oleson KW, Lawrence DM, Bonan GB, Drewniak B, Huang M, Koven CD, Levis S, Li F, Riley WJ,**

1351 **Subin ZM *et al*. 2013.** Technical description of version 4.5 of the Community Land Model (CLM).

1352 NCAR Technical Note NCAR/TN-503+STR. National Center for Atmospheric Research, Boulder,

1353 Colorado. 420 pp.

1354

1355 **Orr DJ, Alcântara A, Kapralov MV, Andralojc PJ, Carmo-Silva E, Parry MAJ. 2016.** Surveying

1356 Rubisco diversity and temperature response to improve crop photosynthetic efficiency. *Plant*

1357 *Physiology*. doi:10.1104/00.16.00750. In Press.

1358

1359 **Ort DR, Long SP. 2014.** Limits on yields in the corn belt. *Science* **344**: 483-484.

1360

1361 **Raddatz T, Reick CH, Knorr W, Kattge J, Roeckner E, Schnur R, Schnitzler K-G, Wetzel P,**

1362 **Jungclaus J. 2007.** Will the tropical land biosphere dominate the climate–carbon cycle feedback

1363 during the twenty-first century? *Climate Dynamics* **29:** 565–574.

1364

1365 **Reich PB. 2014.** The world-wide 'fast-slow' plant economics spectrum: a traits manifesto.

1366 *Journal of Ecology* **102:** 275-301.

1367

1368 **Rogers A. 2014.** The use and misuse of $V_{c,max}$ in Earth System Models. *Photosynthesis Research*

1369 **119**: 15-29.

1370

1371 **Rogers A, Ainsworth EA, Leakey ADB. 2009.** Will elevated carbon dioxide concentration amplify

1372 the benefits of nitrogen fixation in legumes? *Plant Physiology* **151**: 1009-1016.

1373

1374 **Rogers A, Fischer BU, Bryant J, Frehner M, Blum H, Raines CA, Long SP. 1998.** Acclimation of

1375 photosynthesis to elevated CO_2 under low-nitrogen nutrition is affected by the capacity for

1376 assimilate utilization. Perennial ryegrass under free-air CO_2 enrichment. *Plant Physiology* **118**:

1377 683-689.

1378

1379 **Rogers A, Humphries SW. 2000.** A mechanistic evaluation of photosynthetic acclimation at

1380 elevated CO_2. *Global Change Biology* **6**: 1005-1011.

1381

1382 **Salvucci ME, Crafts-Brandner SJ. 2004a.** Inhibition of photosynthesis by heat stress: the

1383 activation state of Rubisco as a limiting factor in photosynthesis. *Physiologia Plantarum* **120**:

1384 179-186.

1385

1386 **Salvucci ME, Crafts-Brandner SJ. 2004b.** Relationship between the heat tolerance of

1387 photosynthesis and the thermal stability of rubisco activase in plants from contrasting thermal

1388 environments. *Plant Physiology* **134**: 1460-1470.

1389

1390 **Sage RF, Sharkey TD. 1987.** The effect of temperature on the occurance of O_2 and CO_2

1391 insensitive photosynthesis in field-grown plants. *Plant Physiology* **84**: 658-664.

1392

1393 **Sage RF, Kubien DS. 2007.** The temperature response of C_3 and C_4 photosynthesis. *Plant Cell &*

1394 *Environment* **30:** 1086-1106

1395

1396 **Sands PJ. 1995a.** Modelling canopy production. I. Optimal distribution of photosynthetic

1397 resources. *Australian Journal of Plant Physiology* **22:** 593-601.

1398

1399 **Sands PJ. 1995b.** Modelling canopy production. II. From single-leaf photosynthetic parameters

1400 to daily canopy photosynthesis. *Australian Journal of Plant Physiology* **22:** 603-614.

1401

1402 **Sands PJ. 1996.** Modelling canopy production. III. Canopy light-utilisation efficiency and its

1403 sensitivity to physiological and environmental variables. *Australian Journal of Plant Physiology*

1404 **23:** 103-114.

1405

1406   **Sato H, Kumagai TO, Takahashi A, Katul GG. 2015.** Effects of different representations of

1407   stomatal conductance response to humidity across the African continent under warmer CO2-

1408   enriched climate conditions. *Journal of Geophysical Research-Biogeosciences* **120**: 979-988.

1409

1410   **Sauter A, Davies WJ, Hartung W. 2001.** The long-distance abscisic acid signal in the droughted

1411   plant: the fate of the hormone on its way from root to shoot. *Journal of Experimental Botany*

1412   **52:** 1991–1997.

1413

1414   **Scafaro AP, Yamori W, Carmo-Silva AE, Salvucci ME, Von Caemmerer S, Atwell BJ. 2012.**

1415   Rubisco activity is associated with photosynthetic thermotolerance in a wild rice (*Oryza*

1416   *meridionalis*). *Physiologia Plantarum* **146:** 99-109.

1417

1418   **Scheiter S, Langan L, Higgins SI. 2013.** Next-generation dynamic global vegetation models:

1419   learning from community ecology. *New Phytologist* **198:** 957-969.

1420

1421   **Serbin SP, Dillaway DN, Kruger EL, Townsend PA. 2012.** Leaf optical properties reflect variation

1422   in photosynthetic metabolism and its sensitivity to temperature. *Journal of Experimental*

1423   *Botany* **63**: 489-502.

1424

1425   **Serbin SP, Singh A, McNeil BE, Kingdon CC, Townsend PA. 2014.** Spectroscopic determination

1426   of leaf morphological and biochemical traits for northern temperate and boreal tree species.

1427   *Ecological Applications* **24:** 1651-1669.

1428

1429   **Sharkey TD. 1985.** Photosynthesis in intact leaves of C-3 plants - physics, physiology and rate

1430   limitations. *Botanical Review* **51**: 53-105.

1431

1432   **Shiklomanov AN, Dietze MC, Viskari T, Townsend PA, Serbin SP. 2016.** Quantifying the

1433   influences of spectral resolution on uncertainty in leaf trait estimates through a Bayesian

1434   approach to RTM inversion. *Remote Sensing of Environment* **183:** 226-238.

1435

1436   **Singh A, Serbin SP, McNeil BE, Kingdon CC, Townsend PA. 2015.** Imaging spectroscopy

1437   algorithms for mapping canopy foliar chemical and morphological traits and their uncertainties.

1438   *Ecological Applications* **25:** 2180-2197

1439

1440   **Shugart HH, Asner GP, Fischer R, Huth A, Knapp N, Le Toan T, Shuman JK. 2015.** Computer and

1441   remote-sensing infrastructure to enhance large-scale testing of individual-based forest models.

1442   *Frontiers in Ecology and the Environment* **13:** 503-511.

1443

1444   **Singsaas EL, Ort DR, Delucia EH. 2001.** Variation in measured values of photosynthetic

1445   quantum yield in ecophysiological studies. *Oecologia* **128:** 15-23.

1446

1447   **Slatyer RO, Ferrar PJ. 1977.** Altitudinal variation in the photosynthetic characteristics of snow

1448   gum, *Eucalyptus paucijlora* Sieb. Ex. Spreng. V. Rate of acclimation to an altered growth

1449   environment. *Australian Journal of Plant Physiology* **4:** 595-609

1450

1451 **Slot M, Garcia MN, Winter K. 2016.** Temperature response of CO_2 exchange in three tropical

1452 tree species. *Functional Plant Biology*, **43:** 468-478.

1453

1454 **Smith NG, Dukes JS. 2013.** Plant respiration and photosynthesis in global-scale models:

1455 incorporating acclimation to temperature and CO_2. *Global Change Biology* **19**:45-63.

1456

1457 **Smith NG, Malyshev SL, Shevliakova E, Kattge J, Dukes JS. 2016.** Foliar temperature

1458 acclimation reduces simulated carbon sensitivity to climate. *Nature Climate Change* **6:** 407

1459

1460 **Stinziano J, Hüner NPA, Way DA. 2015.** Warming delays autumn declines in photosynthetic

1461 capacity in a boreal conifer, Norway spruce (*Picea abies*). *Tree Physiology* **35:** 1303-1313*.*

1462

1463 **Stoy PC, Trowbridge AM, Bauerle WL. 2014.** Controls on seasonal patterns of maximum

1464 ecosystem carbon uptake and canopy-scale photosynthetic light response: contributions from

1465 both temperature and photoperiod. *Photosynthesis Research* **119:** 49-64.

1466

1467 **Suits NS, Denning AS, Berry JA, Still CJ, Kaduk J, Miller JB, Baker IT. 2005.** Simulation of carbon

1468 isotope discrimination of the terrestrial biosphere. *Global Biogeochemical Cycles* **19:** B1017.

1469

1470 **Sun Y, Gu LH, Dickinson RE, Pallardy SG, Baker J, Cao YH, DaMatta FM, Dong XJ, Ellsworth DS,**

1471 **Van Goethem D. 2014.** Asymmetrical effects of mesophyll conductance on fundamental

1472   photosynthetic parameters and their relationships estimated from leaf gas exchange

1473   measurements. *Plant Cell & Environment* **37**: 978-994.

1474

1475   **Tardieu F, Davies WJ. 1993.** Integration of hydraulic and chemical signaling in the control of

1476   stomatal conductance and water status of droughted plants. *Plant Cell & Environment* **16:** 341-

1477   349.

1478

1479   **Teskey R, Wertin T, Bauweraerts I, Ameye M, Mcguire MA, Steppe K. 2015.** Responses of tree

1480   species to heat waves and extreme heat events. *Plant Cell & Environment* **38**: 1699-1712.

1481

1482   **Tholen D, Ethier G, Genty B, Pepin S, Zhu XG. 2012.** Variable mesophyll conductance revisited:

1483   theoretical background and experimental implications. *Plant Cell & Environment* **35**: 2087-2103.

1484

1485   **Thum T, Aalto T, Laurila T, Aurela M, Kolari P, Hari P. 2007.** Parametrization of two

1486   photosynthesis models at the canopy scale in a northern boreal Scots pine forest. *Tellus Series*

1487   *B-Chemical and Physical Meteorology* **59:** 874-890.

1488

1489   **Tuzet A, Perrier A, Leuning R. 2003.** A coupled model of stomatal conductance, photosynthesis

1490   and transpiration. *Plant Cell & Environment* **26**: 1097-1116.

1491

1492 **Twine TE, Bryant JJ, Richter K, Bernacchi CJ, Mcconnaughay KD, Morris SJ, Leakey ADB. 2013.**

1493 Impacts of elevated CO_2 concentration on the productivity and surface energy budget of the

1494 soybean and maize agroecosystem in the Midwest USA. *Global Change Biology* **19**: 2838-2852.

1495

1496 **van Bodegom PM, Douma JC, Verheijen LM. 2014.** A fully traits-based approach to modeling

1497 global vegetation distribution. *Proceedings of the National Academy of Sciences of the United*

1498 *States of America* **111**: 13733-13738.

1499

1500 **von Caemmerer S. 2000.** *Biochemical models of leaf photosynthesis* (vol. 2). CSIRO Publishing,

1501 Collingwood, Australia.

1502

1503 **von Caemmerer S, Evans JR. 1991.** Determination of the average partial pressure of CO_2 in

1504 chloroplast from leaves of several C_3 plants. *Australian Journal Plant Physiology* **18**: 287-305.

1505

1506 **von Caemmerer S, Evans JR. 2015.** Temperature responses of mesophyll conductance differ

1507 greatly between species. *Plant, Cell & Environment* **38**: 629-637.

1508

1509 **von Caemmerer S, Farquhar GD. 1981.** Some relationships between the biochemistry of

1510 photosynthesis and the gas exchange of leaves. *Planta* **153**: 376-387.

1511

1512   **Wang YP, Leuning R. 1998.** A two-leaf model for canopy conductance, photosynthesis and

1513   partitioning of available energy. I. Model description and comparison with a multi-layered

1514   model. *Agricultural and Forest Meteorology* **91:** 89-111.

1515

1516   **Warren JM, Jensen AM, Medlyn BE, Norby RJ, Tissue DT. 2015.** Carbon dioxide stimulation of

1517   photosynthesis in *Liquidambar styraciflua* is not sustained during a 12-year field experiment.

1518   *Aob Plants* **7**: plu074.

1519

1520   **Way DA, Oren R, Kim H-S, Katul GG. 2011.** How well do stomatal conductance models perform

1521   on closing plant carbon budgets? A test using seedlings grown under current and elevated air

1522   temperatures. *Journal of Geophysical Research: Biogeosciences* **116**: G4.

1523

1524   **Way DA, Montgomery RA. 2015.** Photoperiod constraints on tree phenology, performance and

1525   migration in a warmer world. *Plant, Cell & Environment* **38**: 1725-1736.

1526

1527   **Way DA and Oren R. 2010.** Differential responses to increased growth temperatures between

1528   trees from different functional groups and biomes: A review and synthesis of data. *Tree*

1529   *Physiology* **30:** 669-688.

1530

1531   **Way DA, Yamori W. 2014.** Thermal acclimation of photosynthesis: on the importance of

1532   adjusting our definitions and accounting for thermal acclimation of respiration. *Photosynthesis*

1533   *Research* **119:** 89-100.

1534

1535   **Wilkinson S, Davies WJ. 2002.** ABA-based chemical signalling: the co-ordination of responses to

1536   stress in plants. *Plant, Cell & Environment* **25:** 195–210.

1537

1538   **Williams M, Rastetter EB, Fernandes DN, Goulden ML, Wofsy SC, Shaver GR, Melilo JM,**

1539   **Munger JW, Fan SM, Nadelhoffer KJ. 1996.** Modelling the soil-plant-atmosphere continuum in

1540   a Quercus-Acer stand at Harvard forest: The regulation of stomatal conductance by light,

1541   nitrogen and soil/plant hydraulic properties. *Plant Cell & Environment,* **19**: 911-927.

1542

1543   **Wright IJ, Reich PB, Westoby M, Ackerly DD, Baruch Z, Bongers F, Cavender-Bares J, Chapin T,**

1544   **Cornelissen JHC, Diemer M *et al*. 2004.** The worldwide leaf economics spectrum. *Nature* **428:**

1545   821-827.

1546

1547   **Wu J, Albert LP, Lopes AP, Restrepo-Coupe N, Hayek M, Wiedemann KT, Guan K, Stark SC,**

1548   **Christoffersen B, Prohaska N, *et al*. 2016a.** Leaf development and demography explain

1549   photosynthetic seasonality in Amazon evergreen forests. *Science* **351,** 972-976.

1550

1551   **Wu J, Chavana-Bryant, C, Prohaska, N, Serbin, SP, Guan, K, Albert, L, Yang, X, van Leeuwen,**

1552   **W, Garnello, J, Martins, G, *et al*. 2016b.** Convergence in relations among leaf traits, spectra and

1553   age across diverse canopy environments and two contrasting tropical forests. *New Phytologist*

1554   In Press. DOI: 10.1111/nph.14051.

1555

1556   **Wullschleger SD, Epstein HE, Box EO, Euskirchen ES, Goswami S, Iversen CM, Kattge J, Norby**

1557   **RJ, van Bodegom PM, Xu X. 2014.** Plant functional types in Earth system models: past

1558   experiences and future directions for application of dynamic vegetation models in high-latitude

1559   ecosystems. *Annals of Botany* **114,** 1-16.

1560

1561   **Xu CG, Fisher R, Wullschleger SD, Wilson CJ, Cai M, McDowell NG. 2012.** Toward a mechanistic

1562   modeling of nitrogen limitation on vegetation dynamics. *Plos One* **7**: e37914.

1563

1564   **Yamori W, Hikosaka K, Way DA. 2014.** Temperature response of photosynthesis in C_3, C_4, and

1565   CAM plants: temperature acclimation and temperature adaptation. *Photosynthesis Research*

1566   **119:** 101-117

1567

1568   **Zaehle S, Friend AD. 2010.** Carbon and nitrogen cycle dynamics in the O-CN land surface model:

1569   1. Model description, site-scale evaluation, and sensitivity to parameter estimates. Global

1570   *Biogeochemical Cycles* **24**. GB1005.

1571

1572   **Zaehle S, Medlyn BE, De Kauwe MG, Walker AP, Dietze MC, Hickler T, Luo YQ, Wang YP, El-**

1573   **Masri B, Thornton P** *et al*. **2014.** Evaluation of 11 terrestrial carbon-nitrogen cycle models

1574   against observations from two temperate Free-Air CO_2 Enrichment studies. *New Phytologist*

1575   **202:** 803–822.

1576

1577 **Zhou SX, Duursma RA, Medlyn BE, Kelly JWG, Prentice IC. 2013.** How should we model plant

1578 responses to drought? An analysis of stomatal and non-stomatal responses to water stress.

1579 *Agricultural and Forest Meteorology* **182**: 204-214.

1580

1581 **Ziehn T, Kattge J, Knorr W, Scholze M. 2011.** Improving the predictability of global CO_2

1582 assimilation rates under climate change. *Geophysical Research Letters* **38**:L10404.

Figure Legends

1584

1585 **Figure 1** The response of leaf level (a) and canopy level (b,c,d) photosynthesis (*A*) to

1586 instantaneous quantum flux density (*Q*) for three different values of leaf area index; LAI=1 (b),

1587 LAI=3 (c), and LAI=7 (d) for seven models; BETHY (red), CLM (blue), ED2 (cyan), JSBACH (pink),

1588 JULES (dark green) G'DAY (black), O-CN (green). Plots show responses in standard conditions for

1589 a single plant functional type, a generic temperate broad leaved deciduous tree. Where $V_{c,max}$

1590 is 60 µmol m^{-2} s^{-1}. *VPD* was fixed at 1 kPa, soil moisture content was fixed at field capacity, and

1591 atmospheric [O$_2$] at 210 mmol mol^{-1}, C_a at 380 µmol mol^{-1}. Sunlit upper canopy leaf

1592 temperature was fixed at 25°C.

1593

1594 **Figure 2** The response of leaf level (a,b) and canopy level (LAI =3; c, d) photosynthesis (*A*)

1595 to leaf temperature at two atmospheric [CO$_2$] (380 µmol mol^{-1} a, c and 550µmol mol^{-1} b, d) for

1596 seven models; BETHY (red), CLM (blue), ED2 (cyan), JSBACH (pink), JULES (dark green) G'DAY

1597 (black), O-CN (green). Plots show responses in standard conditions for a single plant functional

1598 type, a temperate broad leaved deciduous tree. Where $V_{c,max}$ is 60 µmol m^{-2} s^{-1}. *VPD* was fixed

1599 at 1 kPa, soil moisture content was fixed at field capacity, and atmospheric [O$_2$] at 210 mmol

1600 mol^{-1}, *Q* at 1500 µmol m^{-2} s^{-1}. Sunlit upper canopy leaf temperature was fixed at 25°C.

1601

1602 **Figure 3** The response of leaf level (a,b) and canopy level (LAI=3; c,d) photosynthesis (*A*)

1603 to atmospheric [CO$_2$] (C_a) in seven models; BETHY (red), CLM (blue), ED2 (cyan), JSBACH (pink),

1604 JULES (dark green) G'DAY (black), O-CN (green). Panels show responses in our standard

1605   conditions for a single plant functional type, a temperate broad leaved deciduous tree where

1606 $V_{c,max}$ = 60 μmol m^{-2} s^{-1} (a,c) and when $V_{c,max}$ = 45 μmol m^{-2} s^{-1} (b, d). The *VPD* was fixed at 1

1607   kPa, soil moisture content at field capacity and *Q* at 1500 μmol m^{-2} s^{-1}, atmospheric [O_2] at 210

1608   mmol mol^{-1} Sunlit upper canopy leaf temperature was fixed at 25°C.

1609

1610   **Figure 4**   The response of leaf level (a) and canopy level, where LAI=3 (b) photosynthesis

1611   (*A*) to vapor pressure deficit (*VPD*) for seven models; BETHY (red), CLM (blue), ED2 (cyan),

1612   JSBACH (pink), JULES (dark green) G'DAY (black), O-CN (green). Plots show responses in

1613   standard conditions for a common plant functional type, a temperate broad leaved deciduous

1614   tree. Where $V_{c,max}$ = 60 μmol m^{-2} s^{-1}. Soil moisture content was fixed at field capacity, *Q* at 1500

1615   μmol m^{-2} s^{-1}, C_a at 380 μmol mol^{-1}, atmospheric [O_2] at 210 mmol mol^{-1} Sunlit upper canopy leaf

1616   temperature was fixed at 25°C.

1617

1618   **Figure 5**   The response of leaf level (a) and canopy level, where LAI=3 (b) photosynthesis

1619   (*A*) to soil water content expressed as a fraction of field capacity for seven models; BETHY (red),

1620   CLM (blue), ED2 (cyan), JSBACH (pink), JULES (dark green) G'DAY (black), O-CN (green). Plots

1621   show responses in standard conditions for a single plant functional type, a temperate broad

1622   leaved deciduous tree. Where $V_{c,max}$ = 60 μmol m^{-2} s^{-1}). *VPD* was fixed at 1 kPa, *Q* at 1500 μmol

1623   m^{-2} s^{-1}, C_a at 380 μmol mol^{-1}, atmospheric [O_2] at 210 mmol mol^{-1} Sunlit upper canopy leaf

1624   temperature was fixed at 25°C.

1625

1626 **Figure 6**   Summary of the main areas of scientific activity required to advance

1627   representation of photosynthesis in Earth System Models.   Blue boxes show areas where

1628   fundamental research is required to advance understanding prior to incorporation into models.

1629   Yellow boxes show areas where model refinement or development is required to improve

1630   process representation. Green boxes highlight areas where data are needed to parameterize

1631   models or are required to evaluate alternative approaches. The numbers in the boxes are keyed

1632   to our recommendations in the text.

Table 1 Model representation of the response of C$_3$ photosynthesis to key environmental variables used for this study.

BETHY	CLM4.5	ED2	G'DAY	JSBACH	JULES	O-CN
Leaf photosynthesis (response to C_a)						
Farquhar et al (1980), no TPU limitation	Farquhar et al (1980), includes TPU limitation and co-limitation from Collatz et al. (1991)	Collatz et al. (1991) and Foley et al. (1996); no TPU limitation	Farquhar et al (1980), no TPU limitation	Farquhar et al (1980), no TPU limitation	Collatz et al. (1991), TPU limitation included	Farquhar type (Farquhar et al 1980) following Kull and Kruijt (1998)
Stomatal conductance (response to atmospheric *VPD*, C_a soil moisture and *A*)						
Minimum of (1) stomatal conductance necessary to realize maximum C_i:C_a and (2) soil water availability (Federer 1982).	Sensitivity to atmospheric *RH*, C_a and *A* from Ball, Woodrow & Berry (1987)\n\nSensitivity to soil moisture is from a beta factor applied to the intercept of the Ball, Woodrow & Berry (1987) model. The beta factor is summed over soil layers, weighted by root fraction in each layer and calculated based on soil moisture content	Sensitivity to atmospheric *VPD*, C_a and *A* from Leuning et al. (1995)\n\nWater supply is proportional to soil moisture ☐ root biomass. If the open stomata demand exceeds supply then g_s is linearly scaled between open and closed stomata.	Sensitivity to atmospheric *VPD*, C_a and *A* from Medlyn et al. (2011)\n\nSensitivity to soil moisture from beta factor applied to the slope of the stomatal response (Medlyn et al. 2011). Soil moisture content is expressed as a fraction of total plant available water and dependent on soil type	Estimates potential *A* for any given condition assuming a maximal C_i:C_a resulting from a maximum potential g_s\n\nWhen soil moisture content falls below 50% of plant available water maximum potential g_s is reduced linearly.	Sensitivity to atmospheric *VPD*, C_a and *A* from modification of Leuning et al (1995) model as proposed by Jacobs (1994)	Non-linear sensitivity to specific humidity deficit and C_i. The latter is necessary because *A* for g_s is evaluated at saturating C_i.\n\nA beta factor is applied to the slope of the stomatal response when soil moisture content falls below 50% of plant available water.
Leaf photosynthesis (response to light)						
Rectangular hyperbola, with realized quantum yield and A_{sat} calculated from Farquhar model	Non-rectangular hyperbola, with realized quantum yield and A_{sat} calculated from Farquhar model	Hyperbolic function, with realized quantum yield and A_{sat} calculated from the Collatz (1991) model, no J_{max} term included	Non-rectangular hyperbola, with realized quantum yield and A_{sat} calculated from Farquhar model	Rectangular hyperbola, with realized quantum yield and A_{sat} calculated from Farquhar model	Hyperbolic function, with realized quantum yield and A_{sat} calculated from the Collatz (1991) model, no J_{max} term included	Explicit separation into light saturated and limited regions: A_{sat} is calculated from Farquhar et al (1980). Light

						limited A is assumed to be proportional to light absorption (Kull and Kruijt, 1998)
Leaf photosynthesis (response to temperature)						
Temperature dependence of kinetic constants follows Bernacchi et al. (2001). $V_{c,max}$ and J_{max} are peaked Arrhenius functions of temperature.	Temperature dependence of kinetic constants follows Bernacchi et al. (2001). $V_{c,max}$ and J_{max} are peaked Arrhenius functions of temperature. TPU has the same temperature response as V_{cmax}.	Follows Collatz et al., (1991) and Foley et al., (1996). The temperature dependent kinetic constants follow a modified Arrhenius function. A phenomenological thermal downscaling of $V_{c,max}$ occurs at low and high temperatures (Medvigy et al., 2009)	Temperature dependence of kinetic constants follows Bernacchi et al. (2001). $V_{c,max}$, J_{max} and R_d are peaked Arrhenius functions (Medlyn et al. 2002).	Temperature dependence of kinetic constants and $V_{c,max}$ follow an Arrhenius function, Γ^* and J_{max} vary linearly with temperature.	Follows Collatz et al. (1991), the temperature dependence of kinetic constants follows a Q_{10} function. $V_{c,max}$ has a peaked temperature function calculated from $V_{c,max}$ at 25°C using vegetation-specific optimal temperature ranges.	Temperature dependence of kinetic constants and $V_{c,max}$ follows Bernacchi et al. (2001). The temperature dependence of J_{max} is derived from June et al. (2004)
Leaf photosynthesis (response to soil moisture content)						
	A beta factor is applied to $V_{c,max}$. The beta factor, calculated based on soil moisture potential, is summed over soil layers, weighted by root fraction in each layer.		A beta factor is applied to J_{max} and $V_{c,max}$. Soil moisture content is expressed as a fraction of total plant available water and dependent on soil type		Potential A is multiplied by a soil water stress factor related to the mean soil moisture concentration in the root zone and the critical and wilting point soil water concentrations.(Cox et al.,1998)	A beta factor reduces $V_{c,max}$ and J_{max} when plant available water <20% (Friend, 2010)
Canopy scaling						
Multiple canopy	The Multi-layer	Cohort-based model	Big-leaf model,	Multiple canopy	Multi-layer canopy	Multiple canopy

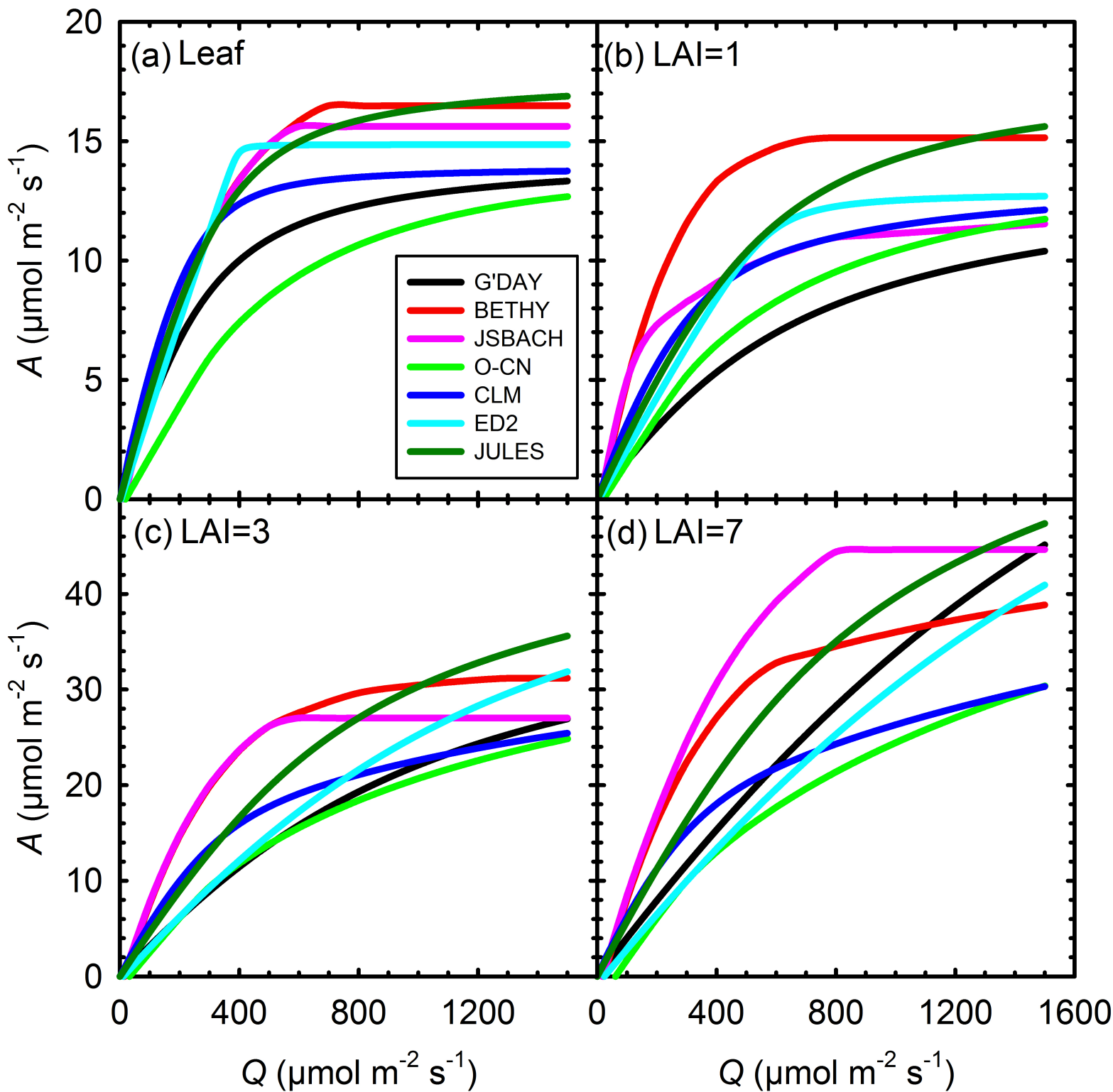|						
layers, using Sellers's (1987) two-stream approximation. $V_{c,max}$ and J_{max} declines exponentially within the canopy following Lloyd et al. (2012).	option explicitly resolves direct and diffuse radiation for sunlit and shaded leaves at each level in the canopy. Both options use Sellers's (1987) two-stream approximation for radiative transfer. Nitrogen declines exponentially with greater cumulative leaf area index.	with the number of layers equal to the number of cohorts. Cohorts differ by PFT definition. Radiation penetration is defined by LAI and the leaf and wood single scattering albedos. There is no separation of sunlit and shaded foliage in the default version	assuming exponential light and nitrogen distributions. Daily A calculated using Gaussian integration (Sands 1996)	layers, using Sellers's (1987) two-stream approximation. LAI typically = 3. For LAI < 3, N (and hence $V_{c,max}$, J_{max}) is distributed evenly in the canopy (assumed to be open). For LAI > 3, N follows the distribution of light (exponential decline).	using the two-stream approximation from Sellers (1985) solving direct and diffuse radiation for sunlit and shaded leaves at each canopy layer. Includes exponential vertical nitrogen distribution of photosynthetic capacity and leaf respiration.	layers with diffuse and direct radiation streams following Spitters (1986). Nitrogen declines exponentially with greater cumulative leaf area index, affecting $V_{c,max}$ and J_{max}
Key Model References						
Knorr & Heimann (2001)	Bonan et al (2011, 2012), Oleson et al (2013)	Medvigy et al (2009), Moorcroft et al (2001)		Knorr & Heimann (2001)	Best et al (2011), Clark et al (2011), Harper (2016)	Zaehle & Friend (2010), Friend (2010)

BETHY = Biosphere Energy Transfer Hydrology scheme, CLM4.5 = the Community Land Model version 4.5, G'DAY = Generic Decomposition And Yield model (G'DAY), JSBACH = Joint Scheme for Biosphere Atmosphere Coupling in Hamburg, JULES = Joint UK Land Environment Simulator, O-CN = An extension of the Organizing Carbon and Hydrology in Dynamic Ecosystems model that includes key N cycle processes.
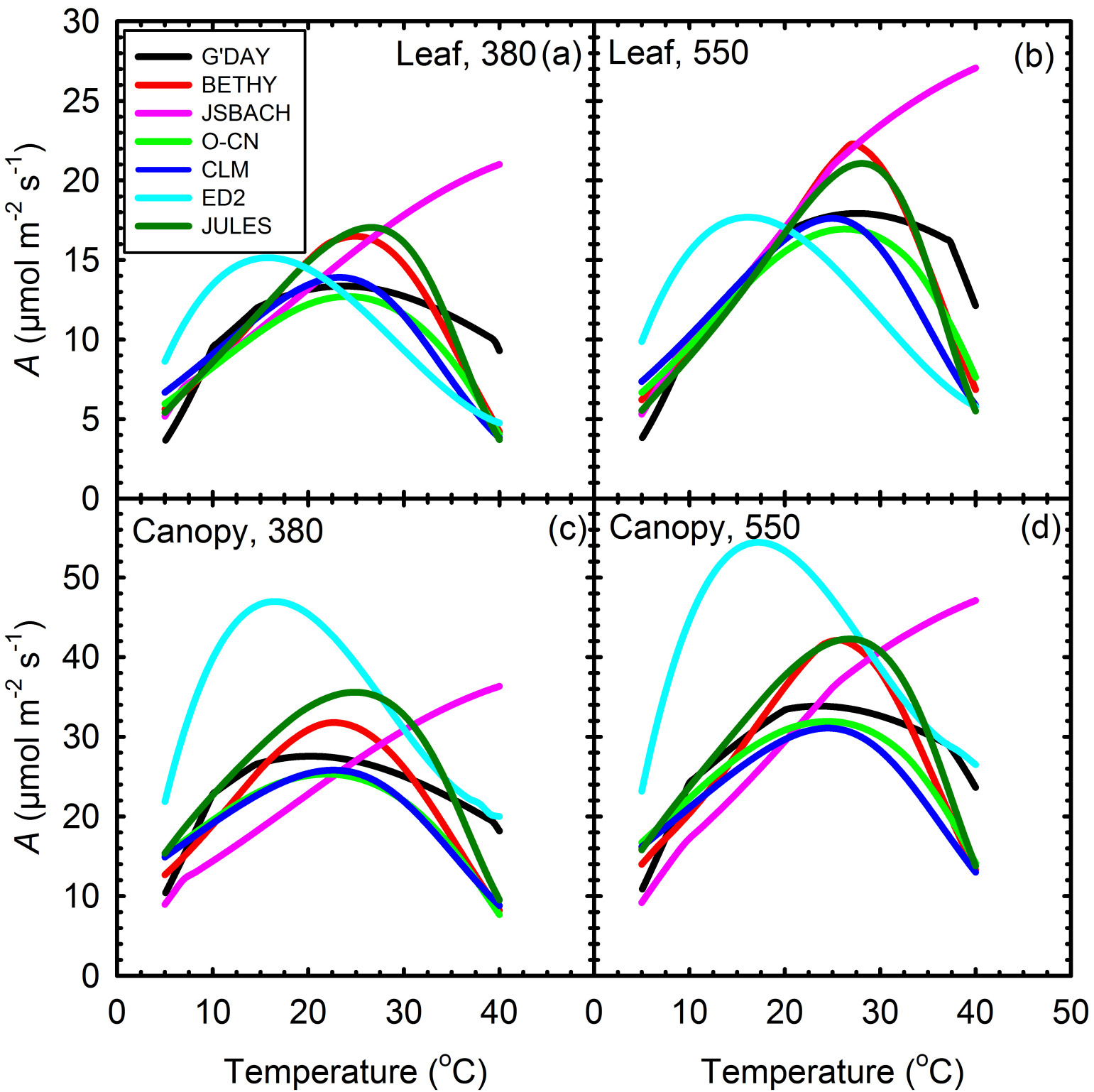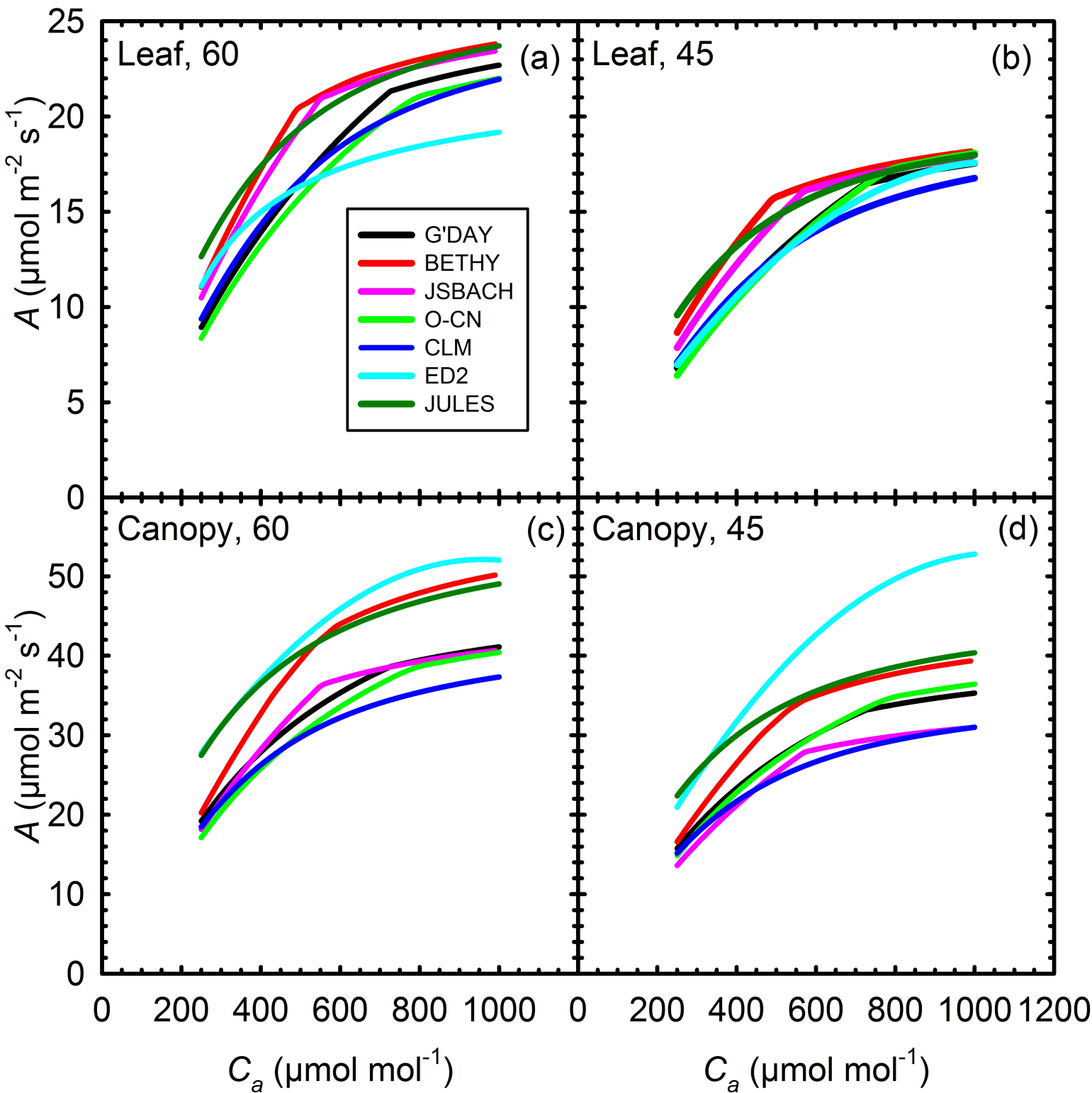
Table 2 Parameters used by the models in this study (Table 1).

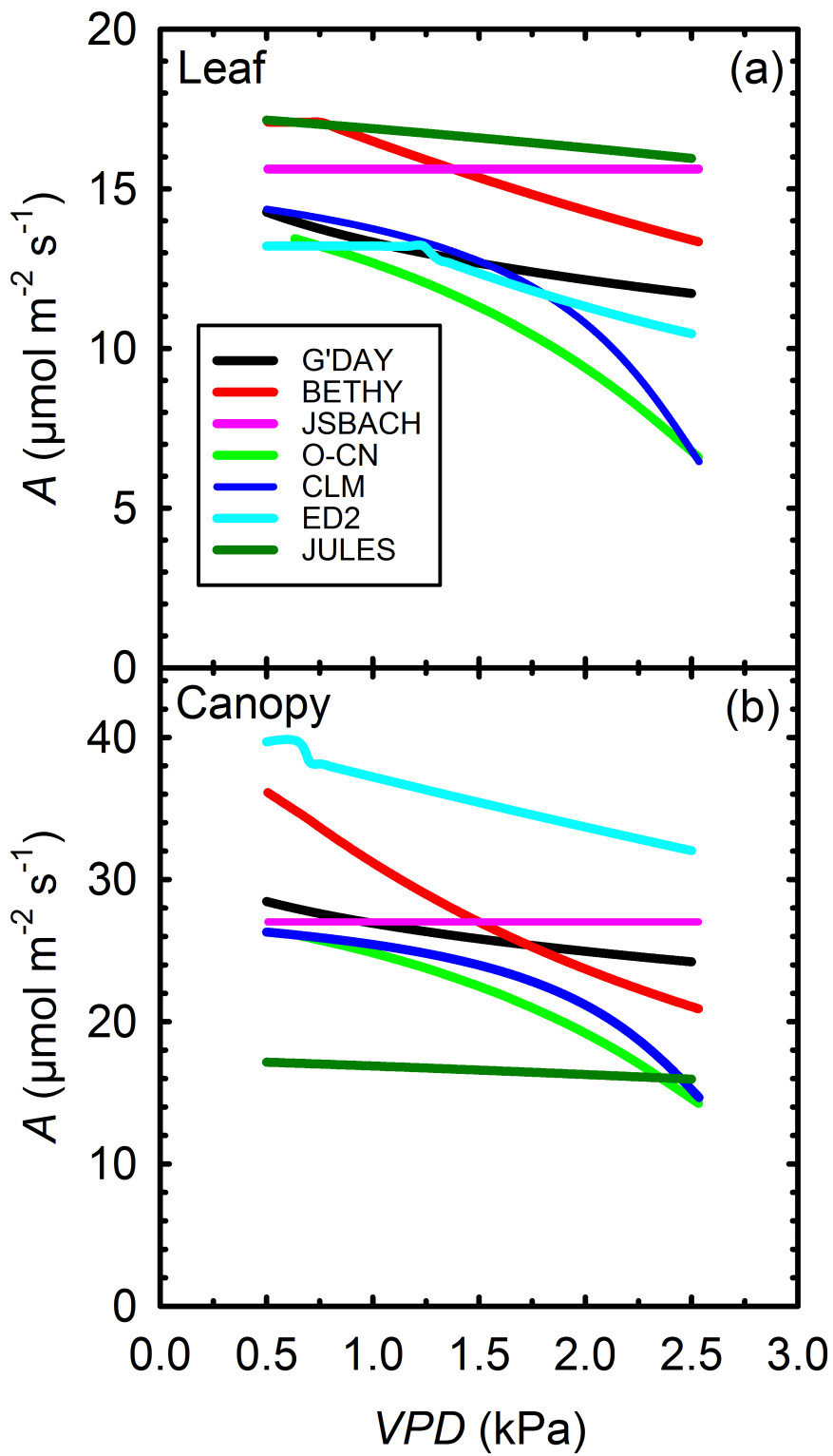|	BETHY	CLM4.5	ED2	G'DAY	JSBACH	JULES	O-CN
K_c at 25°C (µmol mol^{-1})	404.9	404.9	300	404.9	404.9	300	404.9
K_o at 25°C (mmol mol^{-1})	278.4	278.4	294	278.4	278.4	300	278.4
Γ^* at 25°C (µmol mol^{-1})	42.75	42.75	41.57	42.75	42.75	40.38	42.75
Source of kinetic constants	Bern	Bern	Foley	Bern	Bern	Collatz	Bern
JV_{ratio}	1.92	1.97	N.A.	2.00	1.90	N.A.	2.08
J_{max} (µmol m^{-2} s^{-1})	115(86)	115(85)	N.A.	120(90)	114(86)	N.A.	126(94)
Absorbtance	0.88	0.85	0.73	0.85	0.88	0.85	0.80
Convexity	N.A.	0.98 & 0.95[a]	N.A.	0.7	N.A.	0.83 & 0.93[a]	N.A.
C_i at low light (µmol mol^{-1})	348	400	400	293	348	280	N.D.
Model input for quantum yield	0.28[b]	0.4250[b]	0.08[d]	0.26[c]	0.28[b]	0.08[d]	0.08[d]
Calculated ϕ_{int}	0.070	0.106	0.080	0.076	0.070	0.080	0.080
ϕ_{real}	0.049	0.053	0.038	0.038	0.050	0.045	0.022

The Michaelis-Menton constants of Rubisco for carbon dioxide (K_c) and oxygen (K_o), the CO_2 compensation point in the absence of non-photorespiratory michondrial respiration in the light (Γ^*) and the sources of those kinetic constants (Bern = Bernacchi et al. 2001, Collatz = Collatz et al. 1991, Foley = Foley et al. 1996). Where applicable the model specific ratio of the maximum electron transport rate (J_{max}) to maximum photosynthetic capacity ($V_{c,max}$), the (JV_{ratio}), was used to calculate J_{max} for standard conditions, low nitrogen conditions are shown in parentheses. Leaf absorbtance; the convexity term ([a]for the transition between Rubisco and light limited and light limited and TPU limited A respectively); the intercellular [CO_2] (C_i) at low light. Three model inputs were used to parameterize quantum yield ([b]quantum yield of electron transport based on absorbed light, [c]quantum yield of electron transport based on incident light and [d]quantum yield of photosynthesis based on absorbed light and measured under non-photorespiratory conditions (ϕ_{int}). Here we also show the calculated intrinsic quantum yield for all models to enable model comparisons. The modeled realized quantum yield under our standard conditions when $Q = 100$ µmol mol^{-1} (ϕ_{real}) is the initial slope of the leaf level A-Q response shown in Fig 1a for our standard conditions where the ($V_{c,max}$) was set to 60 µmol m^{-2} s^{-1} (and 45 µmol m^{-2} s^{-1} for low nitrogen conditions) and where temperature = 25°C, atmospheric [O_2] = 210 mmol mol^{-1}, C_a = 380 µmol mol^{-1}, VPD = 1 kPa and soil moisture content was at field capacity. N.A. = not applicable, N.D. = no data.

Legend:
- G'DAY
- BETHY
- JSBACH
- O-CN
- CLM
- ED2
- JULES

(a) Leaf, 380

(b) Leaf, 550

(c) Canopy, 380

(d) Canopy, 550

A (μmol m^{-2} s^{-1})

Temperature (^{o}C)

Figure legend:
- G'DAY (black)
- BETHY (red)
- JSBACH (magenta)
- O-CN (green)
- CLM (blue)
- ED2 (cyan)
- JULES (dark green)

(a) Leaf, 60
(b) Leaf, 45
(c) Canopy, 60
(d) Canopy, 45

Y-axis (a, b): A (μmol m^{-2} s^{-1})
Y-axis (c, d): A (μmol m^{-2} s^{-1})
X-axis: C_a (μmol mol^{-1})

(a) Leaf

(b) Canopy

Legend:
- G'DAY
- BETHY
- JSBACH
- O-CN
- CLM
- ED2
- JULES

Y-axis (both panels): A (μmol m^{-2} s^{-1})

X-axis: VPD (kPa)

(a) Leaf

(b) Canopy

Legend:
- G'DAY
- BETHY
- JSBACH
- O-CN
- CLM
- ED2
- JULES

X-axis: Soil Water Content (fraction)

Y-axis (a): A (μmol m^{-2} s^{-1})

Y-axis (b): A (μmol m^{-2} s^{-1})

13 Coupled representation of seasonality in leaf phenology and photosynthetic capacity

21 Remotely sensed data for parameterization and evaluation

19,20 Use existing data to constrain parameterization

18 Radiative transfer

16 Representation of physiological acclimation to elevated CO_2

18 Vertical gradients of canopy architecture, leaf optical properties and photosynthetic variables

2 Light response curves, especially at low temperatures

6 Independent response of stomatal conductance to temperature

17 Discontinue use of single layer big leaf models

1 Mesophyll conductance

8 Use stomatal models that respond to VPD

9 Stomatal slope and intercept

4 Archive raw data

7 Inflection point of CO_2 response

5 Temperature response functions of photosynthetic variables

12 Mechanistic understanding of photoperiod scalars

11 Mechanistic linkage between soil moisture and stomatal conductance

3 Careful, coordinated use of kinetic constants, temperature response functions and approaches

11 Response of photosynthesis and stomatal conductance to drought

10 Use Ψ_{soil} to represent soil water availability
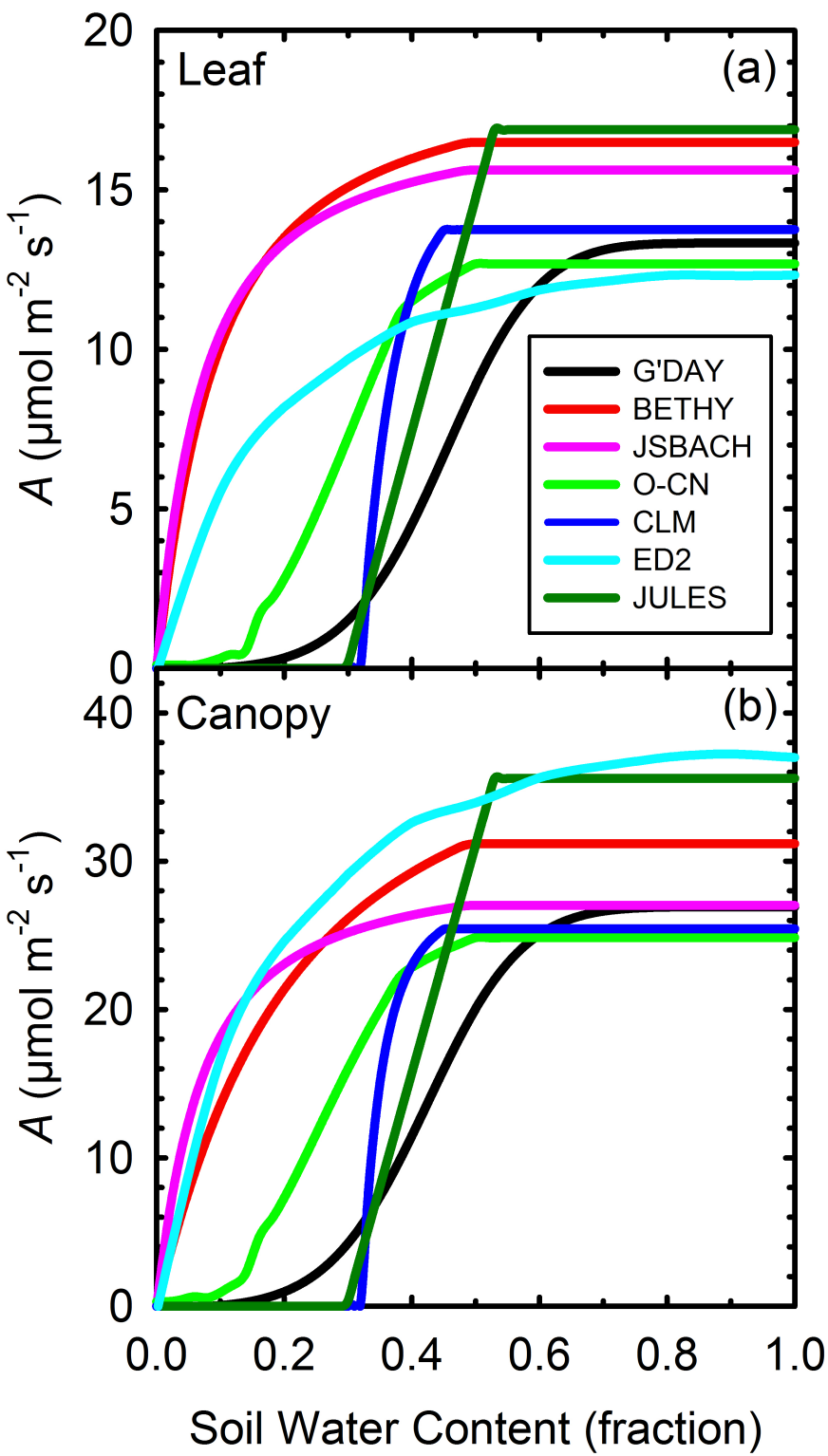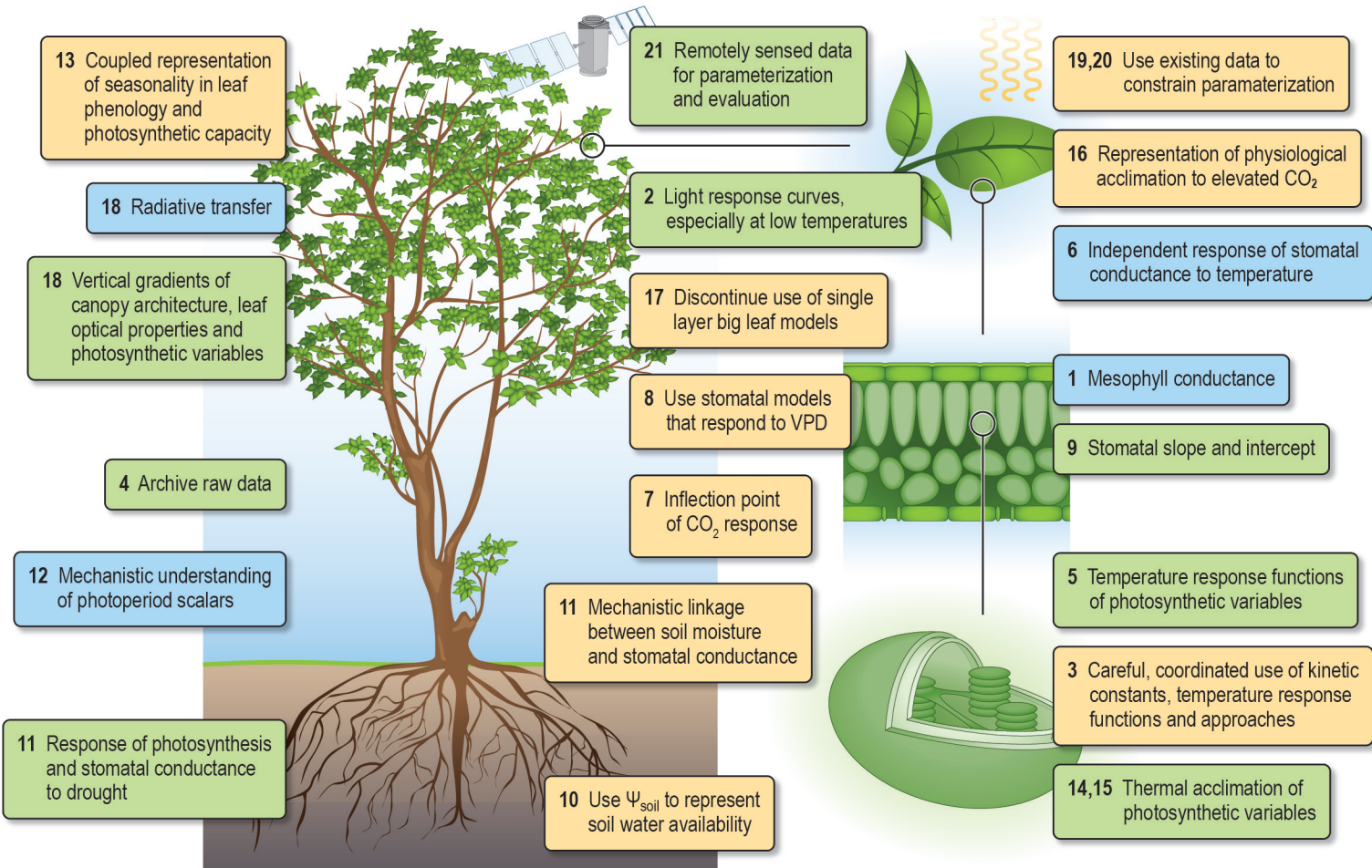
14,15 Thermal acclimation of photosynthetic variables

Data needed for model parameterization or evaluation   Model development activity   Process knowledge required